Function of the Pro-enzyme C-terminal Processing Domain of
Pholiota nameko Tyrosinase

By

Lai Lai Moe

A dissertation submitted to Division of Science for Bio-function development in partial fulfillment
of the requirements for the degree of Doctor of
Bioresources and Environmental Science

Lai Lai Moe

Nationality   : Myanmar

Previous degree   : B. Sc (Hons) Chemistry (Dagon University), Myanmar

                             M. Sc Engineering Chemistry (Dagon University), Myanmar

Laboratory of Food Analysis
Division of Science for Bio-function development
Ishikawa Prefectural University
Nonoichi, Japan
March, 2015

TABLE OF CONTENS

TABLE OF ABBREVIATIONS

PPO	Polyphenol oxidase
TYR	Tyrosinases
CO	Catecholoxidase
L-DOPA	L- 3, 4-dihydroxyphenylalanine
A. bisporus	*Agaricus bisporus*
A. oryzae	*Aspergillus oryzae*
B. megaterium	*Bacillus megaterium*
I. batatas	*Ipomoea batatas*
L. edodes	*Lentinula edodes*
N. crassa	*Neurospora crassa*
O. dofleini	*Octopus dofleini*
P. nameko	*Pholiota nameko*
P. sanguineus	*Pycnoporus sanguineus*
S. castaneoglobisporus	*Streptomyces castaneoglobisporus*
S. glausescens	*Streptomyces glausescens*
T. reesei	*Trichoderma reesei*
V. vinifera	*Verrucomicrobium vinifera*
V. spinosum	*Verrucomicrobium spinosum*
WT	Wild type
E. coli	*Escherichia coli*
LB	Luria-Bertani broth
TP	Tryptone phosphate broth
AEBSF	4-(2-aminoethyl)-benzenesulfonyl fluoride hydrochloride
TBC	*tert*-butylcatechol
ELISA	Enzyme linked immuno sorbent assay
MBTH	3-methyl-2-benzothiazolinone hydrazone hydrochloride hydrate

LIST OF FIGURES AND TABLES

GENERAL INTRODUCTION

Tyrosinases is known to be a key enzyme in the melanogenic pathway that calatyzes the initial rate-determining reaction, the *o*-hydroxylation of monophenols to *o*-diphenols (monophenolase activity or cresolase activity), as well as the oxidation of *o*-diphenols to corresponding *o*-quinones (*o*-diphenolase activity or catecholase activity) (Halaouli *et al.* 2006; Rodriguez-Lopez *et al.* 1992) reducing molecular oxygen to water, both reactions using molecular oxygen (Fig. I). Subsequently, the *o*-quinones undergo non-enzymatic reactions with various nucleophilies, producing intermediates, which associate spontaneously in dark brown pigments (Haghbeen and Tan 2003).
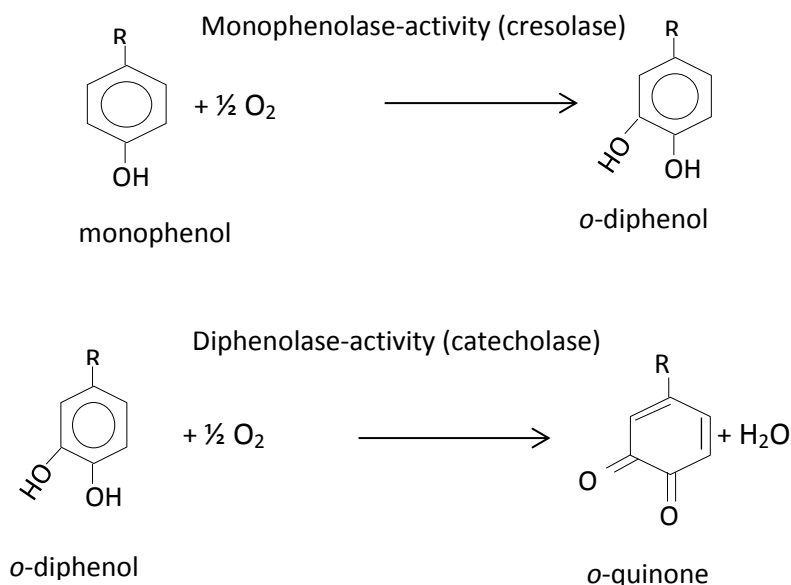
Fig. I Tyrosinase (EC 1.14.18.1) comprises two reactions, the monophenolase and diphenolase activities.

Tyrosinase has the unusual property of catalyzing three distinct reactions within a single biochemical pathway as shown in Fig. II: the hydroxylation of a monophenol (deoxy form), the dehydrogenation of a catechol (oxy form) and the dehydrogenation of a dihydroxyindole (met form). These three states determine the ability of tyrosinase to bind to its substrates and therefore determine the reaction kinetics (Solomon *et al.* 1996). The catalytic mechanisms behind oxidation of a substrate typically involve formation of a

reactive intermediate by the reaction of a reduced Cu ions centre with molecular oxygen, which may also be incorporated to the substrate (Hatcher and Karlin 2004; Rosenzweig and Sazinsky 2006). The met form can bind diphenols and, during the subsequent reaction in which it oxidizes the diphenol and release the *o*-quinone, is converted into the deoxy-form. The deoxy-form is able to bind reversibly with molecular oxygen, producing the oxy-form (Fig. II), which can act on both monophenols and phenols (Fenoll *et al.* 2004).
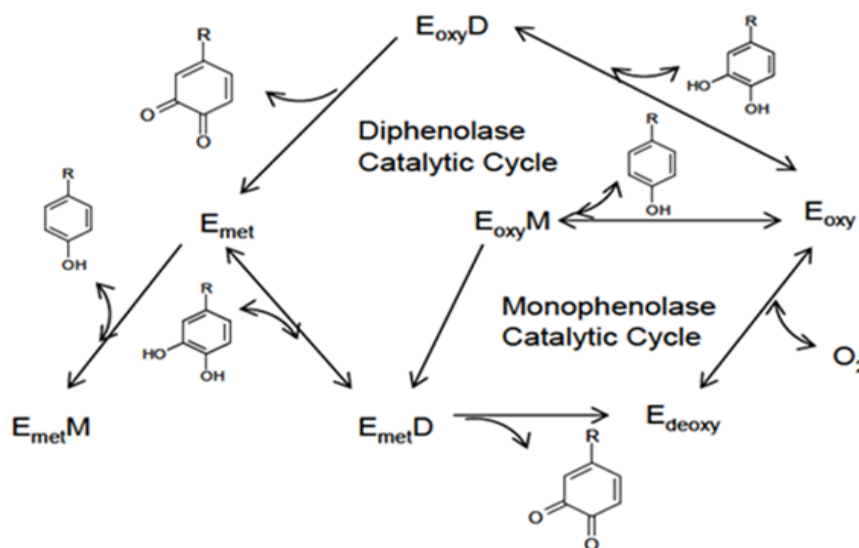
Fig. II Catalytic cycles of the hydroxylation of monophenol and *o*-diphenol to *o*-quinone by tyrosinase (Fenoll *et al* 2004).

Tyrosinase is widely distributed in nature and it can be found in prokaryotic as well as in eukaryotic microbes, in mammals, and wide range of organisms, including bacteria, fungi, plants, insects, and other animals and is responsible for a variety of functions (Halaouli *et al.* 2006; Claus and Decker 2006; Soler-Rivas *et al.* 1999; Westerhof 2006).

In fruits, fungi and vegetables, the melanins are responsible for the browning of wounded tissue when it is exposed to air and the browning occurring during post-harvest storage. In agriculture this poses a significant problem with huge economic impact, making the identification of compounds that inhibit melanin formation extremely important. In other cases (such as raisins, tea and cocoa), the tyrosinase activity is needed for the production of distinct organoleptic properties. In fungi, the role of melanin is correlated with the differentiation of reproductive organs and spore formation, virulence of pathogenic fungi, and tissue protection after injury (Soler-Rivas *et al.* 1999; Hurrell and Finot 1982).

In invertebrates, apart from providing pigmentation, melanin is also involved in three physiologically important processes. These are defense reactions (immunity), wound healing and cuticular hardening (sclerotization). Insects and other arthropods use melanin production as a defensive mechanism to encapsulate foreign organisms. Furthermore, deposition of melanin at a wound site prevents the loss of blood, while the cytotoxic melanogenic quinonoid precursors might kill invading microorganisms at the wound site (Halaouli et al. 2006b).

In mammal, tyrosinase-related melanogenesis is responsible for pigmentation in skin, eye, and hair. Pigmentation contributes an essential part of the protective function of the skin by absorption of UV radiation (Hearing and Tsukamoto 1991; Del Marmol and Beermann 1996). Hyperpigmentation and albinism in mammals are caused by abnormal increase or decrease in tyrosinase activity, respectively (Solano et al. 2006).

Tyrosinase is an attractive enzyme for many applications in biotechnology, food industries, pharmaceutical drugs and environmental technology. The ability of tyrosinases to convert monophenols into diphenols is concerning to the production of antioxidant ortho-diphenols with benefinical properties as food additives or pharmaceutical drugs. The cross linking activity of tyrosinases is due to the non-enzymatic reaction of the oxidised products of tyrosine and other substrate phenols with lysyl, tyrosyl, cysteinyl and histidinyl residues in proteins. Tyrosinases can cross link peptides and proteins in milk, meat and cereals (Aberg et al. 2004; Halaouli et al. 2005; Lantto et al. 2007).

The filamentous fungus T. reesei showed good cross-linking abilities of α-casein proteins as compared to tyrosinases from fungal and plant origins. Tyrosinases from T. reesei and P. sanguineus were found to cross-link α-caseins directly, while tyrosinases from A. bisporus, apple, and potato were capable to cross-link α-caseins only in the presence of L-dopa (Selinheimo et al. 2007a; Selinheimo et al. 2007b). Tyrosinase from A. bisporus has been used for the enzymatic grafting of phenolic moties or proteins onto the chitosan, a polysaccharide biopolymer, obtained mainly from food processing waste water (Aberg et al. 2004). Tailoring properties of polymers, e.g., grafting of silk proteins onto chitosan via tyrosinase reactions has also been reported (Freddi et al. 2006). Tyrosinase catalyzes the oxidation reaction of phenolic compounds, which are highly toxic and hazardous for environment, and it is low cost for processing of water treatment. Tyrosinase is an attractive enzyme also in environmental technology for detoxification of phenol-containing waste water and contaminated soils (Narayan and Agrawal 2012).

Tyrosinases have in common a binuclear type 3 copper centre within their active sites (Hatcher and Karlin 2004; Rosenzweig and Sazinsky 2006; Decker and Terwilliger 2000). The two copper binding regions are called CuA and CuB. These regions each contain three conserved histidine residues, which coordinate to a pair of copper ions in the active site of the enzyme as in Fig. III. This copper pair is the site of interaction of tyrosinase with both

molecular oxygen and its substrates. The CuA and CuB regions share strong homology with the corresponding regions of hemocyanin, which are oxygen carrier found in many molluscs and arthropods and catechol oxidases that oxidize diphenols but do not show the hydroxylation activity (Fenoll *et al.* 2004; Eicken *et al.* 1999). Type-3 copper site can exit in various forms depending on the oxidation state of the Cu ions. These are oxy form, deoxyform and met form (Solomon *et al.* 1996). These proteins also contain a dinuclear copper site and share strong functional, mechanistic and structural similarities with the tyrosinases. Together with the tyrosinase, hemocyanin and catecholase are classified as type-3 copper proteins.
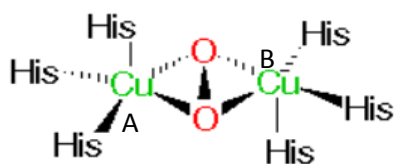
Fig. III Active site of tyrosinase: a binuclear type 3 copper centre.

On the basis of biological source, the monomeric structure of type 3 copper proteins are reorganized to consist of two or three domain regions with different folding motifs: an N-terminal catalytic core domain (central domain), a linker region and a C-terminal domain as in Fig. IV. The N-terminal catalytic core domain contains six conserved histidine residues involved in the coordination of two copper ions. Especially in fungal tyrosinases, the linker region and C-terminal regions are higher sensitivity to proteolysis degradations. In comparison with active domain, the C-terminal domain carried a statistically significant low stability than N-terminal domain (Faccio *et al.* 2013). A tyrosine motif (YXY motif) is a mark of the end of active core domain and the start of the linker region (Flurkey and Inlow 2008). The region between the YXY motif and a tyrosine-glycine motif (YG motif) is a part of the linker region (Faccio *et al.* 2013). The YG motif is not always present in organisms and is especially found in fungal polyphenol oxidase (Garcia-Borron and Solano 2002).

Proteolytic cleavage site

Central domain ～45 kDa   ～20 kDa

N- |yellow| CuA ||| ||| CuB -------- |green| -C   *V.vinifera* PPO*   ⎤ Plant
              |green| *I. batatas* CO*   ⎦

              CuA ||| CuB -------- |green| *A.bisporus* TYR   ⎤ Fungi
              |yellow| CuA ||| CuB -------- |green| *T.reesei* TYR   ⎦

              |yellow| CuA ||| CuB | ORF378 | *S.castaneoglobisporus* TYR*   ⎤
              |yellow| CuA ||| CuB   *B.megaterium* TYR*   ⎥ Bacteria
              |yellow| CuA ||| CuB -------- |green| *V.spinosum* TYR   ⎦
              |yellow| CuA ||| CuB -------- |orange||green| Human TYR   ⎤ Animal

CuA
H$_{A1}$, H$_{A2}$, H$_{A3}$

CuB
H$_{B1}$, H$_{B2}$, H$_{B3}$

Transmembrane region

Signal sequence or
transit peptide

Linker region

Fig. IV Domain organization is representative tyrosinases and catechol oxidases from different organisms. The N-terminal domain is in yellow and diagonal lines indicate the presence of a signal sequence or transit peptide. The central domain is in brown and vertical lines indicate the CuA and CuB sites. The C-terminal domain is in green and in orange shows the presence of a transmembrane region. A deep arrow indicates the cleavage site for the release of the C-terminal domain. The caddie protein ORF 378 co-crystallised with the TYR from *S.castaneoglobisporus* is boxed. Proteins for which the three-dimensional structure is available are marked by an asterisk (for references see Table 1). The molecular masses are approximate and the relative sizes are not scale (Flurkey and Inlow, 2008).

Many tyrosinases from plant, fungal and invertebrate origin exist as latent enzymes which have to be activated *in vivo*. The activation mechanism is still largely unknown, but it has been suggested that an endogeneous protease might be involved in the activation, cleaving off a proteolytic peptide (Espin and Wicher1999). Haemocyanin from *Octopus doflenin* has the C-terminal domain and it has to be acquired polyphenol oxidase activity after proteolytic treatment (Decker *et al* 2007).

In bacterial tyrosinases, the tyrosinase from *Streptomyces castaneoglobisporus* has lacked of C-terminal domain and could be produced in active form only when co-expressed with a second protein of the same operon that favoured the incorporation of copper (Matoba *et al.* 2006). In contrast, the tyrosinases from *Bacillus megaterium and Rhizobium etli*, both lacking the C-terminal domain, could be produced in an active form without the assistance of a caddie protein (Kohashi *et al.* 2004; Cabrera-Valladares *et al.* 2006; Sendovski *et al.*

2011). The lack of the C-terminal is not common to all bacterial tyrosinases and *Verrucomicrobium spinosum* tyrosinase has been reported to contain the C-terminal domain (Fairhead and Thony-Meyer 2010).

The three-dimensional structure of the fungal tyrosinase from *A. bisporus* has been reported, the enzyme mainly adopts α-helical structures, except for the N- and C-terminal β-strands, and the catalytic dinucleur copper center is lodged in a four-helix bundle, where each copper ion (designated as CuA and CuB) is coordinated by three His imidazoles (Ismaya *et al.* 2011). From the crystallographic analysis, core domain of *A. bisporus* exhibited a covalent bond between the ε-carbon atom of one of imidazole ligands and the sulfur atom of cysteine (His-Cys cross-linkage) near the CuA site in the copper center. It was sequence similarly to *Neurospora crassa* tyrosinase. Therefore, fungal tyrsinase might have a thioether bond in the active site (Lerch 1982).

It has been proved that fungal tyrosinase from *A. oryzae*, the apo form of recombinant *melB* tyrosinase (the product of the *melB* gene from *A. oryzae*) can be over-produced from *E. coli*, and that reconstitution of the apo-tyrosinase with the copper (II) ion under aerobic conditions induces the autocatalytic formation of His94-Cys92: cross-linkage in the enzyme active site (His94 is one of the ligands for CuA). Detailed mechanistic analysis has indicated that a (μ-η^2:η^2-peroxo) dicopper (II) species is a key reactive intermediate for the post-translational formation of the His-Cys cross-linkage. The primary structure of the *melB* tyrosinase contains a CuA binding motif consisting of three histidines (His67, His94 and His103) and a CuB binding motif involving three histidines (His328, His332 and His372) and then it is a mark of the end of the active core (copper-binding) domain is the Y-motif. And also noted that the holo-tyrosinase *melB* has no catalytic activity, but after trypsin treatment induced its activity (Nakamura *et al.* 2000).

Report of the crystal structure of *melB* tyrosinase from *A. oryzea* showed the holo-pro- and the apo-pro forms of *melB* tyrosinase at a 1.39 Å and a 2.05 Å resolution, respectively, to provide the first detailed structural information about the fungal tyrosinase containing the C-terminal domain (Fujieda *et al*. 2013b). In the structure (Fig. V), Phe513 residue inhibited the di-copper active centre as the placeholder for the phenolic substrates. The C-terminal domain of *melB* tyrosinase exhibits a seven-stranded antiparalled β-sandwich structure, whose topology is the truncated jellyroll motif. The structural data of holo-pro-form provides important insights into the role of the C-terminal domain not only as a reactively regulation domain but also as a copper chaperone-like machinery.
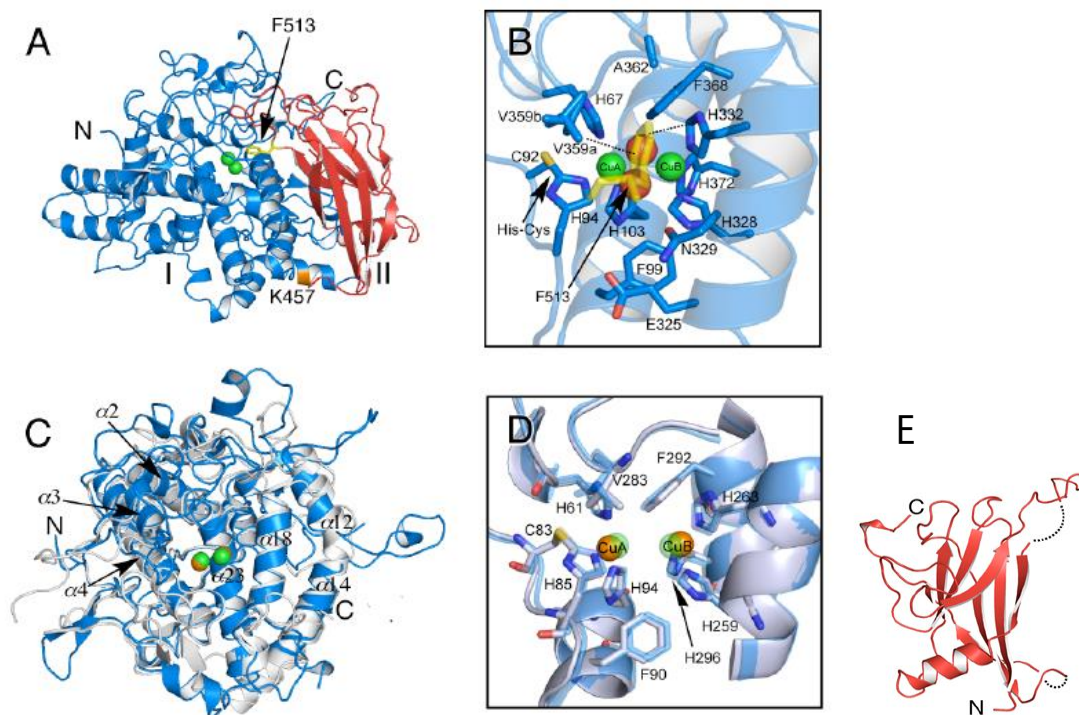
Fig. V Crystal structures of protomer of *melB* holo pro-tyrosinase (A) Structure of the chain A molecule. The copper-binding domain (domain I, Ser1–Phe463) is colored in blue; the *C*-terminal domain (domain II, Gly464–Ala616) in red. Putative proteolytic site (Lys457) is labeled and shown in orange color. The *N*-terminus and *C*-terminus are indicated as N and C, respectively. The black arrow indicates Phe513 from the *C*-terminal domain covering the active site. (B) Active site structure viewing from the *C*-terminal domain. Phe513 is shown as a stick model colored in yellow. Dotted lines indicate closet contacts between atoms. (C) Superimposed structure of the copper-binding domain (blue) vs. mushroom tyrosinase (PDB: 2Y9W) (gray). (D) Superimposed structure of active site structure of *melB* (cyan) vs. *mushroom* tyrosinase (PDB: 2Y9W) (gray). (E) Structure of the C-terminal domain of melB holo-pro-tyrosinase (Fujieda *et al.* 2013b).

Tyrosinase is involved in several biological functions and is mainly responsible for melanins synthesized. Tyrosinase occurs widespread in nature and can be found in all living cells. Research on tyrosinase has been approached from a large number of disciplines, including biophysics, biotechnology, genetics, biochemistry, spectroscopy, medicine and applied chemistry. In spite of the long standing tradition of research on tyrosinase, the relationship between its structure and function remain to be solved to date. The objective of

this study is to understand the relationship between the structure and function of tyrosinase from the mushroom *Pholiota microspora* (synonym *Pholiota nameko*) by using biotechnological techniques.

CHAPTER 1

Recombinant tyrosinase lacking the C-terminal domain

1.1 Introduction

Tyrosinase (EC 1.14.18.1) is a type-3 copper protein, containing a binuclear copper centre and is also known as a polyphenol oxidase. Tyrosinases use molecular oxygen to catalyse the *ortho*-hydroxlation of monophenols (cresolase activity) and the subsequent oxidation of *o*-diphenols (catecholase activity). The resulting *o*-quinones are highly reactive compounds that polymerize non-enzymatically to form melanin pigments (Jolivet *et al.* 1998; Seo *et al.* 2003; Halaouli *et al.* 2006). Tyrosinase is distributed in a wide range of organisms, including bacteria, fungi, plants and insects, and is responsible for various functions including skin pigmentation in mammals, browning and pigmentation reactions in plants and fungi and morphogenesis in fungi (Weaver *et al.* 1970; Jolivet *et al.* 1998; Seo *et al.* 2003; Claus and Decker 2006; Halaouli *et al.* 2006; Wang and Hebert 2006; Westerhof 2006; Largeteau *et al.* 2010). Tyrosinases also confer resistance to pathogens in plants and mediate sclerotization of the cuticle after moulting or injury in arthropods (Sugumaran 2002; Li *et al.* 2009). The cresolase and catecholase activities of tyrosinase can be used for many industrial applications, including detoxification of phenol-contaminated wastewater and soil, pharmaceutical production of *o*-diphenols as drugs and cosmetic production of synthetic melanins for UV protection. In addition, tyrosinase activities improve food flavour and texture by facilitating polymerization of phenol derivatives and cross-linking of protein–protein and protein–polysaccharide complexes (Hurrell and Finot1982; Chen *et al.* 2002; Thalmann and Lötzbeyer 2002; Seo *et al.* 2003; Claus and Decker 2006).

The fungal tyrosinase gene encodes a protein of about 60 kDa comprising an N-terminal catalytic domain of about 40 kDa and a C-terminal domain of about 20 kDa (Wichers *et al.* 2003; Fujieda *et al.* 2013a; Faccio *et al.* 2013; Mauracher *et al.* 2014a). The N-terminal domain contains a pair of coupled copper ions, CuA and CuB, which are coordinated by the six conserved histidine residues HA1, HA2 and HA3 for CuA, and HB1, HB2 and HB3 for CuB. In addition, several highly conserved residues have been identified in the fungal tyrosinase primary structure. These include a conserved arginine residue in the vicinity of the N-terminus, a conserved cysteine residue located two residues before HA2 that is cross-linked with the cysteine residue to form a His-Cys thioether bond, a YXY motif comprising two conserved tyrosine residues that are located C-terminally to HB3, a YG motif comprising conserved tyrosine and glycine residues following the YXY motif and a CXXC motif comprising two conserved cysteine residues in the C-terminal domain.

Isolated fungal tyrosinases have significantly lower molecular weights and lack the C-terminal domain, and cleavage sites have been identified in some fungal tyrosinases (Kupper *et al.* 1989; Espín and Wicher 1999; Halaouli *et al.* 2006b; Selinheimo *et al.* 2006). Sequence similarities of reported cleavage sites indicate a general cleavage site following the YG motif (Fig. 1a; Flurkey and Inlow 2008; Fujieda *et al.* 2013a; Faccio *et al.* 2013). Fungal tyrosinase is expressed as an inactive zymogen pro-tyrosinase, which is post translationally activated by the proteolytic removal of the C-terminal domain (Flurkey and Inlow 2008). Approximately 98% of the tyrosinase present in mushrooms reportedly occurs in the inactive pro-tyrosinase form (Espín and Wicher 1999).

Recently, the crystal structure of a recombinant pro-tyrosinase from *Aspergillus oryzae* showed that the C-terminal domain of pro-tyrosinase shields the active site of tyrosinase, and that the buried active site is exposed following removal of the C-terminal domain (Fujieda *et al.* 2013b). This crystal structure also demonstrated that the C-terminal domain plays an important role in regulating enzyme activity by prohibiting substrate access to the copper centre and avoiding undesirable intracellular reactions of highly reactive *o*-quinones. This report also revealed that three cysteine residues, including one in the His-Cys thioether linkage and two in the CXXC motif, contribute to copper incorporation into the active site, indicating that the C-terminal domain plays crucial roles in both regulation of enzyme activity and in copper incorporation.

Previously, we isolated a tyrosinase of 42 kDa from fruiting bodies of *Pholiota nameko* (nomenclature *Pholiota microspore*; Neda 2008), which is one of the most popular edible mushrooms in Japan and is readily available in large quantities. The purified tyrosinase was truncated at Phe387 and released a 25-kDa C-terminal domain from a 67-kDa pro-tyrosinase (Kawamura-Konishi *et al.* 2007). Thus, we expressed the pro-tyrosinase as a thioredoxin fusion protein in *Escherichia coli* cells and obtained a soluble protein (Fig. 1.1, (i); Kawamura-Konishi *et al.* 2011). Although the catalytic activity of the pro-tyrosinase could not be detected by measuring increases in the absorption of quinone products, proteolytic digestion of the protein using α-chymotrypsin produced an active 44-kDa tyrosinase after truncation of the 25-kDa C-terminal domain (Fig. 1.1, (ii); Kawamura-Konishi *et al.* 2011). Thus, truncation of the C-terminal domain from the pro-tyrosinase activated the N-terminal catalytic domain, suggesting that the C-terminal domain of the *P. nameko* tyrosinase acts as an inhibitor in the pro-enzyme.

In the present chapter, I investigated the role of the C-terminal domain of *P. nameko* tyrosinase by expressing a recombinant 42-kDa tyrosinase lacking the 25-kDa C-terminal domain in *E.coli*.
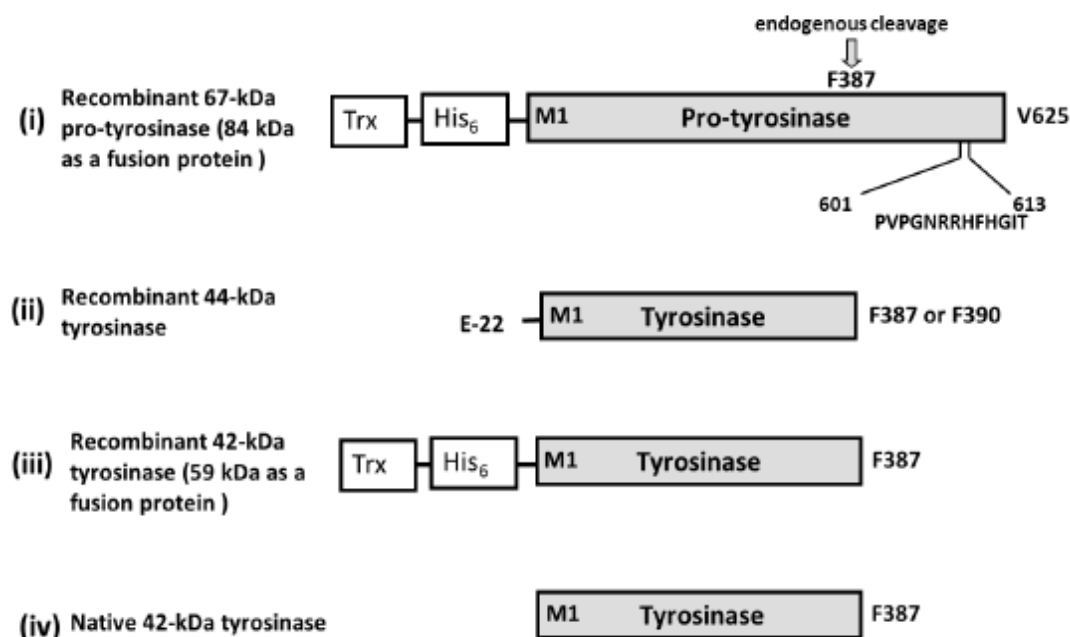
Fig. 1.1 Schematic representations of the present *P. nameko* tyrosinases; (i) The recombinant 67-kDa pro-tyrosinase (84 kDa) comprised thioredoxin (Trx, 12 kDa), His6 tag (His6, 5 kDa) and the encoded pro-tyrosinase (pro-tyrosinase, 67 kDa). The encoded pro-tyrosinase has an N-terminal Met (M1) and a C-terminal Val (V625). The grey arrow represents the endogenous cleavage site at Phe387. The sequence Pro601–Thr613 was used for the preparation of the anti-C antibody. (ii) The recombinant 44-kDa tyrosinase was prepared by digestion of the recombinant 67-kDa pro-tyrosinase with α-chymotrypsin; the N-terminal residue was determined as Glu-22. (iii) The recombinant 42-kDa tyrosinase (59 kDa) comprised thioredoxin (Trx, 12 kDa), His6 tag (His6, 5 kDa) and the encoded tyrosinase (tyrosinase, 42 kDa). (iv) Endogenuos native 42-kDa tyrosinase; Shadowed boxes indicate tyrosinase or pro-tyrosinase; C-terminal residues of the tyrosinases are shown on right.

1.2 Material and methods

1.2.1 Materials

   3-methyl-2-benzothiazolinone hydrazone hydrochloride hydrate (MBTH) was purchased from Sigma-Aldrich (St. Louis, MO, USA), 4-*tert*-butylcatechol (TBC) from Wako Pure Chemical (Osaka, Japan), tyramine from Nacalai Tesque (Kyoto, Japan), 4-(2-

aminoethyl)-benzenesulfonyl fluoride hydrochloride (AEBSF) from Merck (Darmstadt, Germany) and peroxidase-conjugated goat anti-rabbit IgG was purchased from Kirkegaard & Perry Laboratories (Washington, DC, USA). Ni^{2+} Chelating Sepharose ^{TM} Fast Flow was obtained from GE Healthcare (Uppsala, Sweden). Bacto Tryptone, Yeast Extract and Bacto Agar were purchased from Disfco, SDS-PAGE standard Broad Range and Kaleidoscope Prestained Standard were from Bio-Rad Laboratories, Inc. All other reagents were of analytical grade.

1.2.2 Construction of expression vector

DNA fragments for the expression of the 42-kDa tyrosinase lacking the C-terminal sequence (238 amino acids) were amplified using polymerase chain reaction (PCR). *Eco*RV and *Sal*I restriction sites were introduced into the DNA using KOD plus DNA polymerase (Toyobo, Osaka, Japan). The full length tyrosinase cDNA-2 (GenBank accession number AB275647; Kawamura-Konishi *et al.* 2007) was cloned into pUC118 (Merck) and was used as the template. Primer sets included 5′-AGATATCATGTCTCGCGTTGTTATCACTGG-3′ (sense primer; *Eco*RV restriction site is underlined) and 5′-ACGCGTCGACTTAGAAAACCGAAGCTCCG-3′ (antisense primer; *Sal*I restriction site is underlined and a stop codon is shown in italics). The PCR product was cloned into the plasmid pUC118 and the resulting plasmids were treated with *Eco*RV and *Sal*I, and were ligated with the expression vector pET32b(+) (Merck) to create plasmid pTyr42-2. After DNA sequencing, pTyr42-2 was used to transform *E. coli* strain BL21 (DE3; Merck). Subsequently, a 42-kDa tyrosinase containing a His_6 tag and a fusion thioredoxin in the N-terminal segment was expressed using the plasmid pTyr42-2.

1.2.3 Expression of recombinant protein

Transformed cells carrying the pTyr2 plasmid were cultured for 8 h at 37ºC in Luria-Bertani (LB) broth supplemented with 50 μg/ml ampicillin. This culture was used to inoculate Tryptone Phosphate (TP) broth (Moore *et al*. 1993) supplemented with 50 μg/ml ampicillin and 5 mM $CuSO_4$. After incubation for 48 h at 18ºC, the cells were harvested by centrifugation, and the pellet was resuspended in 20 mM Tris-HCl buffer, pH 7.2, and then centrifuged again.

1.2.4 Purification of recombinant protein

The cells were disrupted by addition of BugBuster^{TM} HT (1.5 ml/g of wet cells, Merck) and incubated for 15 min at 26ºC in the presence of the protease inhibitor cocktail for purification of His-tagged proteins (Sigma-Aldrich) with gentle shaking. Next, the cell lysate was centrifuged. Following centrifugation, the clear supernatant was fractionated by 30−60% saturated ammonium sulfate. The protein precipitates were dialysed against buffer

A (10 mM sodium phosphate buffer, pH 7.0, containing 0.5 M NaCl). After centrifugation, the supernatant was loaded onto a Ni^{2+} Chelating Sepharose^{TM} Fast-Flow column (50 ml) equilibrated with buffer A. The column was washed with buffer A and with 50 mM imidazole in buffer A, and the retained proteins were eluted with 0.5 M imidazole in buffer A. The absorbance of the eluate was monitored continuously at 280 nm, and 1-ml fractions were collected. The purity of the fractions was assayed by sodium dodecyl sulfate-polyacrylamide gel electrophoresis (SDS-PAGE). Those fractions containing the pure protein were pooled and dialysed against 50 mM Tris-HCl, pH 7.2. Protein concentration of the dialysed fraction was determined using the Bio-Rad Protein Assay (Bio-Rad Laboratories, Hercules, CA, USA) with bovine serum albumin as the standard.

1.2.5 Electrophoretic analysis

The purity of the recombinant proteins and their molecular masses were assessed by SDS-PAGE under denaturing conditions. Enzyme activity of the recombinant proteins was detected by denaturing SDS-PAGE and SDS-PAGE without boiling or reducing agent. For denaturing SDS-PAGE, samples were boiled in 50 mM Tris-HCl, pH 6.8, 8% (w/v) glycerol, 2% (w/v) SDS and 5% (w/v) 2-mercaptoethanol for 5 min and then electrophoresed at room temperature. For SDS-PAGE without boiling or reducing agent, samples in 50 mM Tris-HCl, pH 6.8, 8% (w/v) glycerol and 0.1% (w/v) SDS were not boiled and were electrophoresed at 4°C. In both cases, the electrophoresis was performed on 10% polyacrylamide gels at 20 mA for 80 min according to the method of Laemmli (Laemmli 1970). Appropriate molecular mass standards were used in all cases. Protein bands were stained with Coomassie Brilliant Blue R-250 staining solution. Enzyme activity on the gel was visualized by incubation with 1 mM tyramine and 1 mM MBTH in 50mM acetate buffer, pH 5.0, containing 0.1% (w/v) SDS and 2% (v/v) *N, N*-dimethylformamide after washing with the same buffer (Espín *et al*. 1997).

1.2.6 Western blot analysis

Rabbit sera containing polyclonal antibodies elicited against tyrosinase purified from fruiting bodies of *P. microspora* (Kawamura-Konishi *et al*. 2007) or a peptide of PVPGNRRHFHGIT were prepared using custom service from Scrum Co. (Tokyo, Japan). The peptide sequence was one of the epitope sequences presented by the company. Protein bands from the gels were electro-transferred at 4ºC onto a PVDF membrane (Bio-Rad). The membrane was incubated with 2% skim milk in PBS for 60 min and then washed three times with washing buffer [PBS containing 0.05% (w/v) Tween 20]. For detection of tyrosinase, the membrane was incubated with 0.01 mg/ml rabbit tyrosinase antibodies for 30 min at room temperature. The membrane was washed with the washing buffer and then incubated with secondary goat anti-rabbit IgG conjugated with peroxidase. For detection of

proteins with the His$_6$ tag, the membrane was incubated with anti-His$_6$ tag antibodies conjugated with peroxidase (Qiagen, Hilden, Germany) for 1 h at room temperature. In all cases, 4-methyl-1-naphtol and H$_2$O$_2$ were used as substrates for peroxidase to detect immunoreactive bands.

1.2.7 Copper analysis

Copper concentrations of protein samples were determined using a Polarized Zeeman Atomic Absorption Spectrophotometer Z-2000 (Hitachi-hitec). A calibration curve of copper ions was generated using copper ion standard solutions of 10, 20, 30 and 40 ppb, and concentrations were occasionally determined with ICP-MS using a custom service from Ishikawa Health Service Association (Ishikawa, Japan).

1.3 Results and discussion

To investigate the role of the C-terminal domain of *P. nameko* tyrosinase, a recombinant 42-kDa *P. nameko* tyrosinase lacking the C-terminal peptide after Phe 387 was expressed as a fusion protein (Fig. 1.1, (iii)). Because insufficient quantities of the soluble protein were purified from *E. coli* cells, the partially purified protein fraction was analysed using SDS-PAGE (lane 5, Fig. 1.2 (A)). Among CBB stained bands on the gel, a band of approximately 59 kDa corresponded to the calculated value of the fusion protein. Thus, further western blot analyses of the protein fraction were performed using anti-TYR and anti-C antibodies, which were raised against a 42-kDa tyrosinase from fruiting bodies (Fig. 1.1, (iv)) or the Pro601-Thr613 peptide from the C-terminal region of the encoded pro-tyrosinase (Fig. 1.1 (i)), respectively. Although the anti-TYR antibody detected a band of approximately 59 kDa (lane 5 in Fig. 1.3 (A)), no bands were detected with the anti-C antibody (lane 5 in Fig. 1.3 (B)), indicating that the recombinant 42-kDa tyrosinase was expressed as a fusion protein in the soluble fraction of *E. coli* cells. Catalytic activities for *t*-butyl catechol were not detected by measuring absorption increases of the *t*-butyl quinone in the partially purified protein fraction (data not shown). Thus, to detect enzyme activity in the protein fraction, SDS-PAGE was performed without boiling and in the absence of reducing agents, and the gel was reacted with a substrate of tyramine in the presence of nucleophilic MBTH, which reacts with quinone from tyramine and forms a stable chromogenic adduct. This method has higher sensitivity for tyrosinase activity than measurements of quinone absorption. No bands were detected from protein fractions, whereas a coloured band was clearly observed for the recombinant 67-kDa pro-tyrosinase, which was used as a positive control (Figure 1.3 (B), lanes 5 and 1, respectively). These

data indicate that the recombinant tyrosinase lacking C-terminal domain has no activity. It is a copper deficiency.
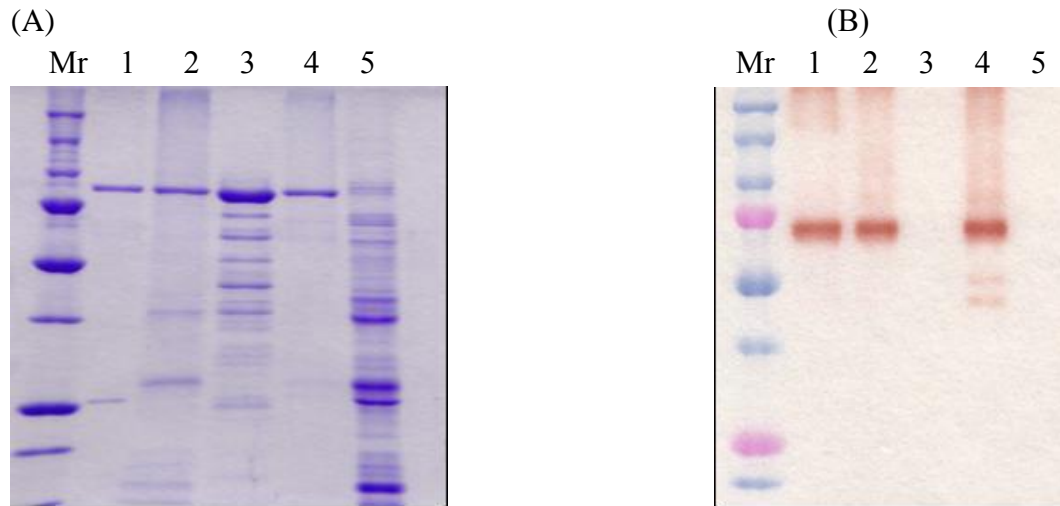
Fig. 1.2 SDS-PAGE of recombinant pro-tyrosinases (lane 1) and tyrosinase (lane 5). (A): CBB staining; (B): activity staining; (Mr): molecular weight marker.
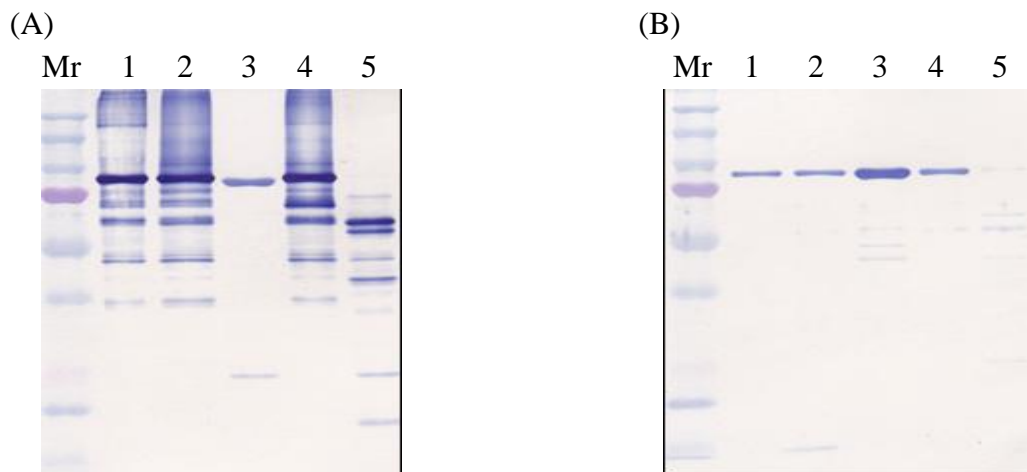
Fig. 1.3 Western blots of recombinant pro-tyrosinases (lane 1) and tyrosinase (lane 5). (A): Anti-tyrosinase immunoglobulin binding activity; (B): anti-C-terminal immunoglobulin binding activity; (Mr): molecular weight marker.

1.4 Conclusion

In this chapter, the results showed that recombinant tyrosinase lacking the 25-kDa C-terminal domain is a copper deficiency and non-active form. Therefore, it is concluded that the C-terminal domain is not only inhibitor but also essential for the catalytic activity of the N-terminal domain of *P. nameko* tyrosinase.

CHAPTER 2

Site-directed mutagenesis on the C-terminal domain of pro-tyrosinase

2.1 Introduction

As presented in Chapter 1, the C-terminal domain is essential for the catalytic activity of the N-terminal domain of *P. nameko* tyrosinase. In Chapter 2, to identify amino acid residues on the C-terminal domain that affect the catalytic activity of the N-terminal domain of pro-tyrosinase, site-directed mutagenesis experiments were performed. Four mutants of the recombinant pro-tyrosinase were prepared, including a His_6 tag and a thioredoxin fusion proteins F515G (Phe515 was substituted with glycine), H539N (His539 was substituted with asparagine), L540G (Leu540 was substituted with glycine) and Y543G (Tyr543 was substituted with glycine). In this study the recombinant 67-kDa pro-tyrosinase was used as a positive control.

The location of Phe515 residue on the C-terminal domain of *P.nameko* tyrosinase was selected by comparing with similar alignment sequences of the reported crystal structure of *Aspergillus oryzae* tyrosinase and *P. nameko* tyrosinase sequence. The position of F513 residue of *A. oryzae* tyrosinase is located at the tip of the C-terminal domain and its phenyl ring stacks onto the imidazole ring of one of the CuB ligands. Furtheremore its side chain is accommodated just above the dinuclear copper centre as the "placeholder" for phenolic substrates (Fujieda *et al.* 2013b). Leu540 residue exists as a substrate-binding pocket of active site and prevents the substrate access. Its functions as a competitive inhibitor likes the reported *Streptomyces* species, bacteria tyrosinase complex with caddie protein Tyr98 of ORF378 (Matoba *et al.* 2006). We selected H539 residue as a mutation site because its imidazole ring may affect to the active site. In mutant Y543G, its phenyl ring may affect to the active site. These residues are in the vicinity of the Leu540 residue.

For the investigation of the mutants, I proceeded in purification of the mutant, proteolytic digestion of the C-terminal domain, measurement of the activity, and copper content determination. Four kinds of mutant on the C-terminal domain of tyrosinase are F515G, H539N, Y543G and L540G. To identify properties of the mutants, I performed denaturing SDS-PAGE, non-denaturing SDS-PAGE and western blotting analysis by using two specific antibodies. Furthermore I analysed the kinetic activities and Cu content in each mutant.

2.2 Materials and methods

2.2.1 Materials

Resource Q and HiTrap Phenyl HP columns were obtained from GE Healthcare (Uppsala, Sweden). Other reagents were described in chapter 1.

2.2.2 Site-directed mutagenesis of the pro-tyrosinase

Oligonucleotide-directed mutagenesis experiments were performed using pTyr2 plasmid (Kawamura-Konishi *et al*. 2011) as a template. Mutant clones were generated using a QuickChange Site-Directed Mutagenesis Kit (Stratagene, La Jolla, CA, USA) according to the supplier's protocol. Primer sequences for site-directed mutagenesis included F515G, sense primer 5′-GGCGCCCATCACGCCGGCGTCAACAGCGCCGCAG-3′, antisense primer 5′-CTGCGGCGCTGTTGACGCCGGCGTGATGGGCGCC-3′; H539N, sense primer 5′-GTGGTCGAAGGCTTCGTCAATCTGACTAAATACATTTCT-3′, antisense primer 5′-AGAAATGTATTTAGTCAGATTGACGAAGCCTTCGACCAC-3′; L540G, sense primer 5′-GGTCGAAGGCTTCGTCCATGGCACTAAATACATTTCTGAGC-3′, antisense primer 5′-GCTCAGAAATGTATTTAGTGCCATGGACGAAGCCTTCGACC-3′; Y543G, sense primer 5′-CGTCCATCTGACTAAAGGCATTTCTGAGCATGCTG -3′, antisense primer 5′-CAGCATGCTCAGAAATGCCTTTAGTCAGATGGACG -3′ (Codons corresponding with changed amino acid residues are underlined). All cloning manipulations were confirmed by nucleotide sequencing of the coding region in the mutated pTyr2, which was used to transform *E. coli* strain BL21 (DE3). Mutant pro-tyrosinases containing a His_6 tag and a fusion thioredoxin in the N-terminal segment were expressed using the resulting plasmids.

2.2.3 Expression and purification of the fusion proteins of the mutants

Mutated proteins were expressed as fusion proteins in *E. coli* cells cultured in Tryptone Phosphate broth (Moore *et al*. 1993) supplemented with 50 μg/ml ampicillin and 5 mM $CuSO_4$ and purified using a Ni^{2+} Chelating Sepharose Fast-Flow column according to a previous study (Kawamura-Konishi *et al*. 2011). Protein concentrations were determined using Bio-Rad Protein Assay kits (Bio-Rad Laboratories, Hercules, CA, USA) with bovine serum albumin as a standard. Further purification was performed for the mutant F515G using a HiTrap Q ion-exchange column (1 ml) in 20 mM Tris-HCl (pH 8.2) with a NaCl concentration gradient of 0.3–0.5 M and a Phenyl Sepharose Hi Trap HIC column (1 ml) in 50 mM sodium phosphate buffer (pH 7.0) containing 1.0 M ammonium sulphate with an ammonium sulphate concentration gradient of 1.0–0 M.

2.2.4 Digestion of the fusion protein using α-chymotrypsin

The purified fusion protein (0.14 mg/ml) was digested with bovine pancreatic α-

chymotrypsin (0.04 mg/ml, Sigma-Aldrich) in buffer B (10 mM Tris-HCl, pH 7.4) at 23°C. AEBSF (2 mM) was added to the reaction mixture to terminate the reaction. For subsequent purification, 30% saturated ammonium sulfate was added to the reaction mixture and the reaction mixture was applied to a HiTrap Phenyl HP column (5 mL × 2) in buffer B containing 30% saturated ammonium sulfate. Adsorbed proteins were eluted with an ammonium sulfate linear gradient (30−0% saturation in 3 column volumes) in buffer B. Activity assays were carried out in 50 mM sodium acetate buffer, pH 5.0, containing 2 mM tyramine, 2 mM MBTH, 2% N, N-dimethylformamide and 0.1% (w/v) SDS (Espín et al. 1997). The reaction was carried out for 5 min at room temperature and the absorbance at 415 nm was measured after the addition of 1 M perchloric acid to terminate the reaction. Active fractions were pooled and the protein concentration of the pooled fraction was determined using the Bio-Rad Protein Assay with bovine serum albumin as the standard.

2.2.5 Electrophoretic analysis

The procedure is the same as in chapter 1.

2.2.6 Western blot analysis

The procedure is the same as in chapter 1.

2.2.7 Copper analysis

The procedure is the same as in chapter 1.

2.2.8 Kinetic analysis of tyrosinase reaction

Tyrosinase activity was assayed at 25°C by monitoring the increase in absorbance of t-butyl-quinone at 400 nm [$\varepsilon = 1,150$ M^{-1}cm^{-1} (Rodriguez-López et al. 1992)] in 25 mM Tris-HCl, pH 7.2, containing 200 μM TBC. Assays were initiated by the addition of the enzyme. Kinetic parameters of the enzyme were obtained by assaying the enzyme activity at different TBC concentrations. Kinetic data were analysed by Michaelis−Menten kinetics as described previously (Kawamura-Konishi et al. 2007).

2.3 Results and discussion

2.3.1 Purification of recombinant pro-tyrosinase

Wild type pro-tyrosinase

Wild type recombinant pro-tyrosinase, TYR67, the full length of $P.$ $nameko$ tyrosinase was expressed in $E.$ $coli$ as N-terminal fusion products with 12-kDa thioredoxin (Trx) and 5-kDa His-tag$_6$. It was accumulated as a soluble fraction in $E.$ $coli$ and the molecular mass

of the recombinant fusion protein was approximately 84-kDa. For expression of wild type (WT) recombinant pro-tyrosinase in *E. coli*, 28.89 g/L of proteins were yielded in shaking-flask cultures. The WT pro-tyrosinase was purified by one step purification procedure using Ni^{2+} chelating (Hi Trap Chelating) column chromatography (Fig. 2.1) with 500 mM imidazole solution.

The purified WT pro-form had an 84-kDa of major protein band observed in the result of denaturing SDS-PAGE (Fig. 2.5A), which was in agreement with the calculated molecular mass of the fusion protein. A 70-kDa of tyrosinase positive color band was observed on the gel of non-denaturing SDS-PAGE (Fig. 2.5B). 84-kDa bands were detected in the results of Western blot analysis by using anti-tyrosinase antibodies and anti-C-terminal antibodies (Figs. 2.6A and B).

Based on these data, purified WT pro-tyrosinase had similar properties to native tyrosinase (Kawamura-Konishi *et al.* 2011) and it was confirmed that the WT pro-tyrosinase was produced as the fusion protein with an 84-kDa molecular mass.
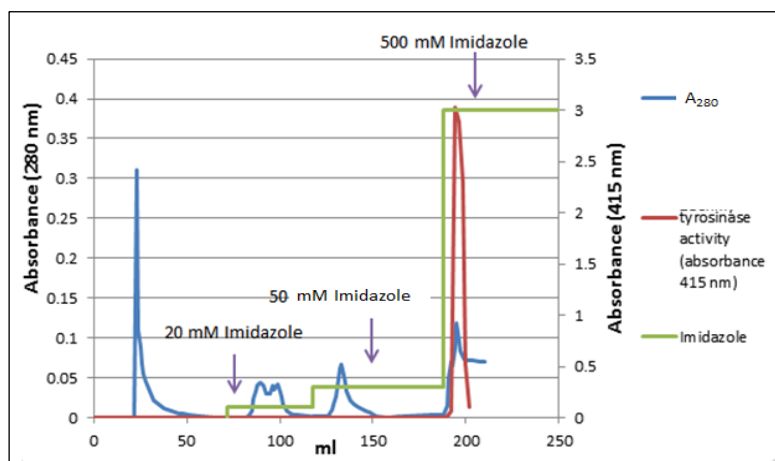
Fig. 2.1 Chromatogram of wild type recombinant pro-tyrosinase purified by a Ni^{2+} chelating column.

Pro-tyrosinase mutant F515G

The expression of mutant F515G pro-form was prerformed using *E. coli* expression system, which yielded 2.55 g/L of proteins in shaking-flask cultures. This mutant was purified with a two-step purification procedure, consisting of Hi Trap Q Ion exchanged column chromatography and Phenyl sepharose Hi Trap HIC column chromatography (Figs. 2.2A and B).

The purified F515G pro-tyrosinase showed an 84-kDa of major protein band on the denaturing SDS-PAGE gel (Fig. 2.5A), and did not show color band with tyrosinase-

activity on the gel of non-denaturing SDS-PAGE (Fig. 2.5B). However, 84-kDa bands were observed in the results of western blot analysis by using anti-tyrosinase and anti-C-terminal antibodies (Figs. 2.6A and B).

These results suggested that mutant F515G pro-tyrosinase had a mass of fusion protein but different properties from WT pro-tyrosinase and other mutants as shown below. The purification of this mutant was very difficult and purification yield was very low. The mutant could not be purified by Ni^{2+} chelating column chromatography with different concentrations of imidazole. And then I used the Hi Trap Q Ion exchange column with various concentrations of NaCl but could not purufy this mutant. Therefore, I performed next step purification using Phenyl sepharose Hi Trap HIC column and purified this mutant. The purified mutant was observed as an 84-kDa fusion protein.

From the experiments, I obtained informations about this mutant, that is, the property of mutant F515G was much different from that of WT, Hi Trap HP Ni^{2+} Chelating Column was not useful for purification of mutant F515G, and NaCl concentration between 0.3 M and 0.5M was effective for elution of mutant F515G from Hi Trap Q Ion exchange column.
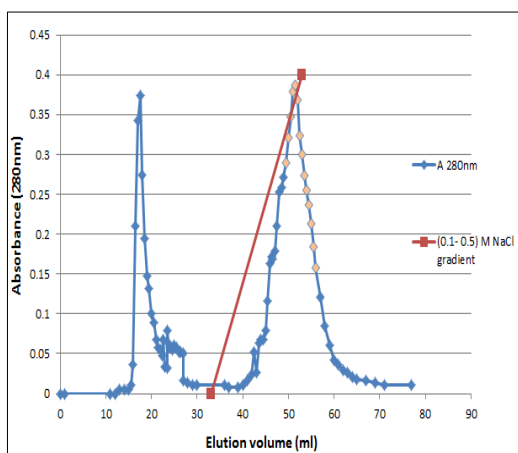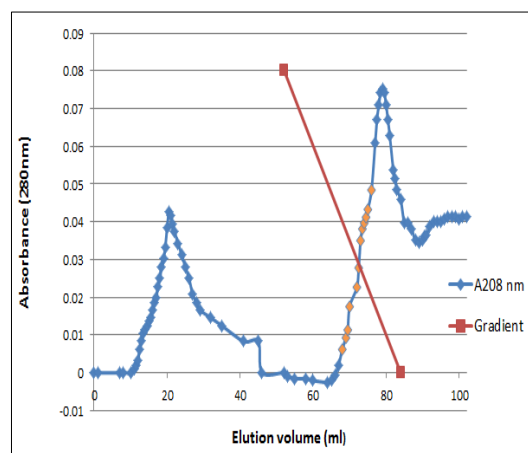
(A)   (B)

Fig. 2.2 Purification of mutant F515G pro-tyrosinase: (A) Hi Trap Q Ion exchange column chromatography; (B) Phenyl Sepharose Hi Trap HIC column chromatography.

Pro-tyrosinase mutant H539N

The expression of mutant H539N pro-form was performed in *E. coli* stain BL21, yieldsing 30.38 g/L of proteins in shaking-flask culture. The mutant H539N was purified by

one step purification procedure with Ni^{2+} chelating (Hi Trap Chelating) column chromatography (Fig. 2.3).

The purified H539N was observed as an 84-kDa band in the result of denaturing SDS-PAGE of method (Fig. 2.5A), which was in agreement with the calculated molecular mass of the fusion protein. About 70-kDa tyrosinase-activity positive band was shown in from the non-denaturing SDS-PAGE (Fig. 2.5B). 84-kDa bands were observed in the results of western blotting analysis using anti-tyrosinase and anti-C-terminal antibodies (Figs. 2.6A, and B, respectively).These results indicated that mutant H539N had similar properties to WT pro-tyrosinase and confirmed that the mutant was generated as a fusion protein with an 84 kDa molecular mass.
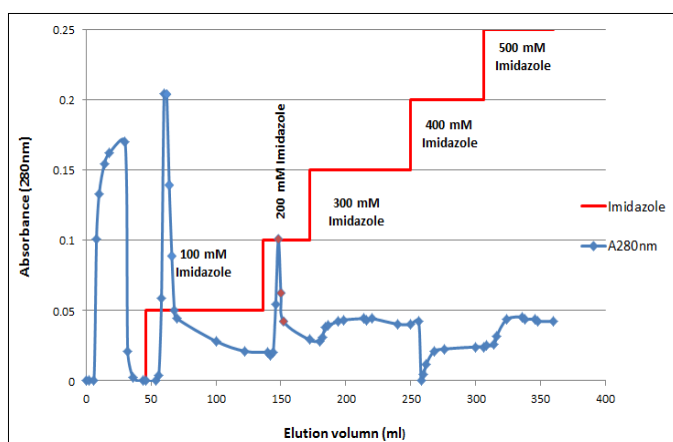
Fig. 2.3 Purification of mutant H539N pro-tyrosinase using a Ni^{2+} chelating column.

Pro-tyrosinase mutant Y543G

In the fermentation of the expression of mutant Y543G pro-form, *E. coli* cell culture using shaking-flask yielded 30.38 g/L of protein. The Y543G was purified by one step purification procedure with a Ni^{2+} chelating (Hi Trap Chelating) column (Fig. 2.4).

The purified Y543G was observed as an 84 kDa protein band on denaturing SDS-PAGE gel (Fig. 2.5A), which molecular mass was in agreement with the calculated one of the corresponding fusion protein. An activity staining band of 70-kDa was shown in the non-denaturing SDS-PAGE analysis (Fig. 2.5B). 84-kDa bands were detected in the results of western blot analysis using anti-tyrosinase and anti-C-terminal antibodies (Figs. 2.6A and B, respectively).

Based on these results, Y543G pro-tyrosinase had similar properties to the WT pro-tyrosinase, and it was confirmed that the mutant was generated as a fusion protein of 84 kDa molecular mass.
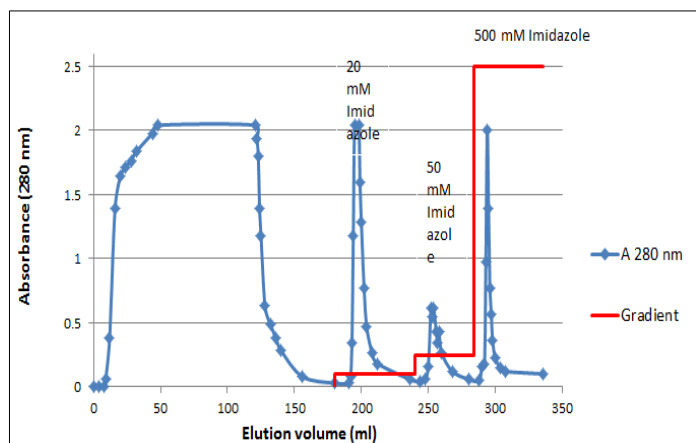
Fig. 2.4 Chromatogram for purification of Y543G pro-tyrosinase using a Ni^{2+} chelating column.

CBB   Activity staining
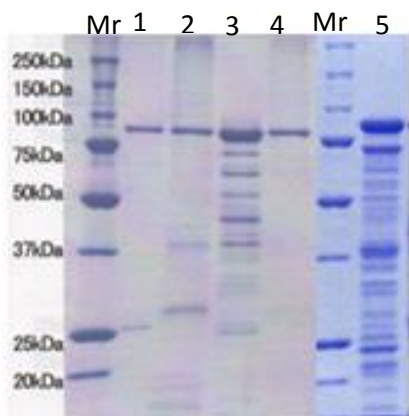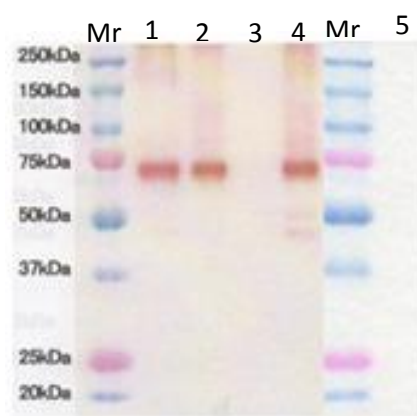
(A)   (B)

Fig. 2.5 SDS-PAGE of recombinant pro-tyrosinases by CBB staining (A) and activity staining (B). Molecular mass marker (Mr); WT (1); H539N (2); L540G (3); Y543G (4); and F515G(5).

23

Anti-TYR

Anti-C

(A)
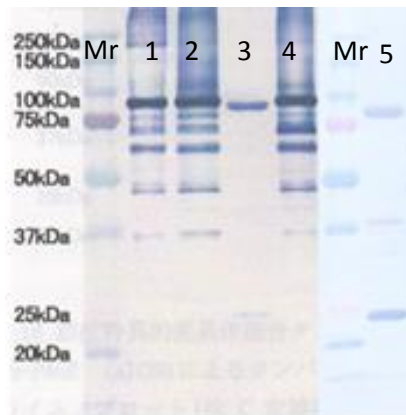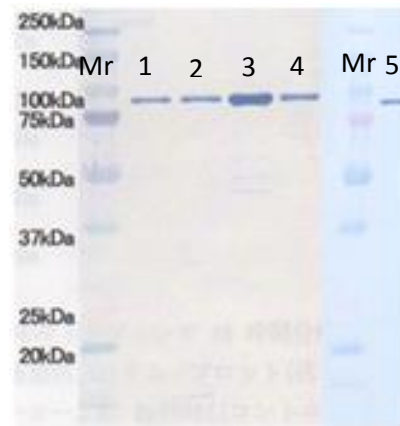
(B)

Fig. 2.6 Western blots of recombinant pro-tyrosinases using specific antibodies: anti-tyrosinase (A) and anti-C-terminal (B). Molecular mass marker (Mr); WT (1); H539N (2); L540G (3); Y543G (4); and F515G(5).

2.3.2 Alpha chymotrypsin digestion of recombinant pro-tyrosinase mutants

The pro-form of WT was digested at C-terminal cleavage site by bovine pancreatic α-chymotrypsin for overnight incubation. After the digestion, a 44 kDa tyrosinase was observed in the result of denaturing SDS-PAGE (Fig. 2.10A) and it showed tyrosinase activity on the gel of non-denaturing SDS-PAGE (Fig. 2.10B). In western blot analysis, anti-tyrosinase antibody reacted the 44-kDa band but anti-C one did not (Figs. 2.11A and B, respectively). These results indicated that the obtained 44-kDa protein was the same as the reported 44-kDa tyrosinase (Kawamura-Konishi *et al*., 2007).

F515G mutant could not be activated by bovine pancreatic α-chymotrypsin digestion and 44 kDa band of tyrosinase was not observed in incubation time from 0.5 hr to overnight (Fig. 2.7). After overnight incubation, F515G had 25 kDa molecular mass as shown in the result of denaturing SDS-PAGE (Fig. 2.10A) and tyrosinase activity was not observed on the gel of non-denaturing SDS-PAGE (Fig. 2.10B). Moreover, western blotting analysis did note detect the 25 kDa of protein with anti-tyrosinase and anti-C-terminal antibodies (Fig. 2.11A and B, respectively). F515G may have unfolded structure because chymotrypsin can digest easily inner parts of the mutant form (Faccio *et al*., 2013), indicating that this mutant had a different conformation from other mutants.

H539N was digested at C-terminal cleavage site by bovine pancreatic α-chymotrypsin for overnight incubation. After the proteolytic degrading, the resultant active tyrosinase was purified by Phenyl Sepharose Hi Trap HIC column chromatography. The protein was observed as a 44 kDa band in the result of denaturing SDS-PAGE (Fig. 2.10A) and tyrosinase positive color band on the gel of non-denaturing SDS-PAGE (Fig. 2.10B). Western blot analysis showed a 44-kDa band with anti-tyrosinase antibody but did not with anti-C antibody (Fig. 2.11A and B, respectively). These results agreed with WT tyrosinase (Kawamura-Konishi *et al.*, 2007). From the time course of chymotrypsin digestion of this mutant, overnight incubation gave only the 44-kDa form (Fig. 2.8)

Y543G was digested at C-terminal cleavage site by bovine pancreatic α-chymotrypsin. From the time course of the digestion, two hours incubation gave a 44-kDa form (Fig. 2.9). After the digestion, the 44-kDa form was purified by Phenyl Sepharose Hi Trap HIC column chromatography. The protein was confirmed as 44 kDa of molecular mass in the result of denaturing SDS-PAGE (Fig. 2.10A) and a tyrosinase positive color band on the gel of non-denaturing SDS-PAGE (Fig. 2.10B). Aanti-tyrosinase antibody reacted with the 44-kDa protein band but anti-C antibody did not (Fig. 2.11A and B, respectively). These results agreed with WT tyrosinase (Kawamura-Konishi *et al.*, 2007).
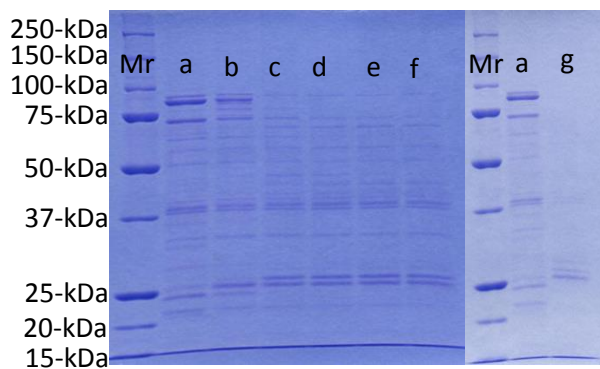
Fig. 2.7 Times course of digestion of F515G mutant with α chymotrypsin. Molecular weight marker (Mr); incubation time, (a): 0 h; (b): 0.5 h; (c): 1 h; (d): 1.5 h; (e): 2.0 h; (f) and (g): overnight.
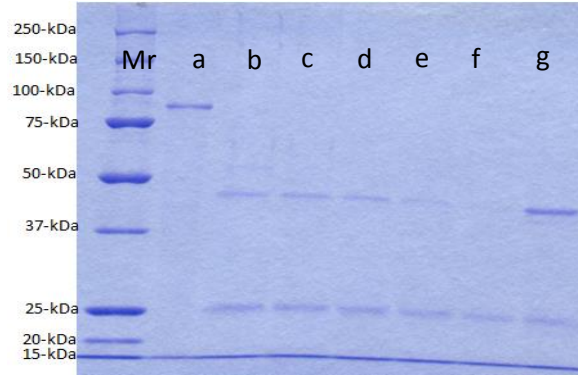
Fig. 2.8 Times course of digestion of H539N mutant with α chymotrypsin. Molecular weight marker (Mr); incubation time, (a): 0 h; (b): 0.5 h; (c): 1 h; (d): 1.5 h; (e): 2.0 h; (f) and (g): overnight.
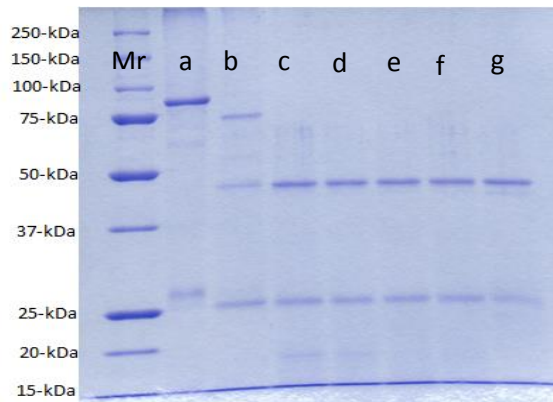
Fig. 2.9 Times course of digestion of Y543G mutant with α chymotrypsin. Molecular weight marker (Mr); incubation time, (a): 0 h; (b): 0.5 h; (c): 1 h; (d): 1.5 h; (e): 2.0 h; (f) and (g): overnight.
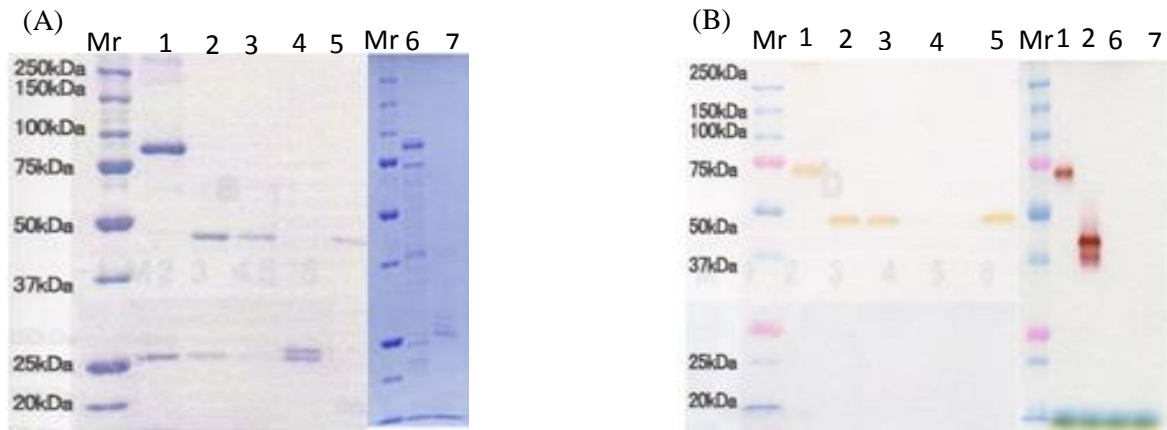
Fig. 2.10 SDS-PAGE of recombinant tyrosinases. (A): CBB staining; (B): Activity staining. Molecular weight marker: (Mr); WT pro-tyrosinase: (1); tyrosinases from WT pro-tyrosinase: (2); form H539N: (3); from Y543G: (4); from L540G: (5); from F515G : (6); from F515G: (7).
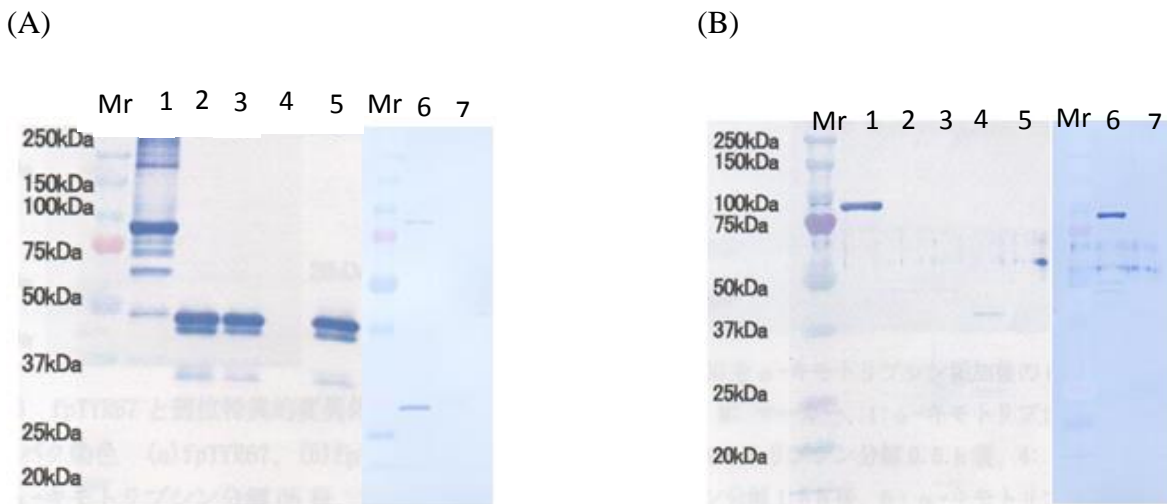
Fig. 2.11 Western blots of recombinant tyrosinases. Anti-tyrosinase (A) and (B) anti-C-terminal (B) antibodies were used. Molecular weight marker: (Mr); WT pro-tyrosinase: (1); tyrosinases from WT pro-tyrosinase: (2); form H539N: (3); from Y543G: (4); from L540G: (5); from F515G : (6); from F515G: (7).

2.3.3 Enzymatic activity of recombinant tyrosinae from the mutants

In order to study the effect of the enzyme concentration upon the reaction rate, we used 200μM of 4-*tert*-butylcatechol as a substrate with different enzyme concentrations (Fig. 2.12). The 44-kDa form from H539N showed higher activity than that form Y543G. Values of kinetic parameters, K_m and k_{cat}, were determined according to Michaelis-Menten kinetics from the double reciprocal plots (Fig. 2.13). The 44-kDa tyrosinase from WT showed a higher activity than those form H539N and Y543G, and the former showed a lower activity than the latter.

The 44-kDa tyrosinase from WT exhibited a specific activity of 0.92 U/mg and k_{cat}/K_m value of 0.86μM^{-1}s^{-1}. The former and the latter were 448 and 2.1 times, respectively, lower than tyrosinase purified from fruit bodies. And the 44-kDa tyrosinases from H539N and Y543G were exhibited specific activities of 0.065 and 0.55 U/mg, respectively. The values of k_{cat}/K_m were 0.27 (H539N) and 0.19 μM^{-1}s^{-1} (Y543G), as expressed in table 3. Therefore, specific activity of the 44-kDa tyrosinases from H539N was 14.2 times and that from Y543G was 1.67 times smaller than the 44-kDa tyrosinase from WT. The values of k_{cat}/K_m were 3.2 times (H539N) and 4.5 times (Y543G) smaller than the 44-kDa tyrosinase from WT. In the case of H539H, tentative k_{cat}/K_m value was obtained assuming that K_m value was much larger than the substrate concentration used in experiment. In contrast, F515G mutant showed no enzymatic activity.

From all the results, the 44-kDa tyrosinases from WT, H539N and Y543G have similar structures to the native tyrosinase from *P. nameko* but their enzymatic activities were 2.1, 6.7 and 9.5 times, respectively, and lower than that of the native tyrosinase. The values of the 44-kDa tyrosinases form H539N and Y543G were lower than that of WT (*e.g.* 3.2 and 4.5 times, respectively). The results showed that there are differences in the tyrosinase activities in native enzyme, the 44-kDa tyrosinases from WT and mutatants. It is suggested that the activities of the 44-kDa tyrosinases form the mutatnts were much lower than that from WT, whereas those form F515G and L540G had no activity.
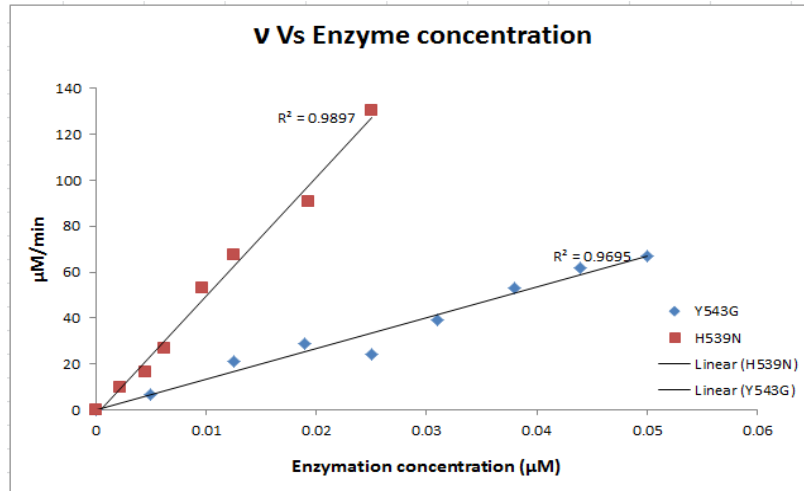
Fig. 2.12 Relationship between the enzyme concentration and the initial velocity at 200 μM TBC and 25 ºC. Diamonds indicate the 44-kDa tyrosinase from Y543G; rectangulars from H539N.
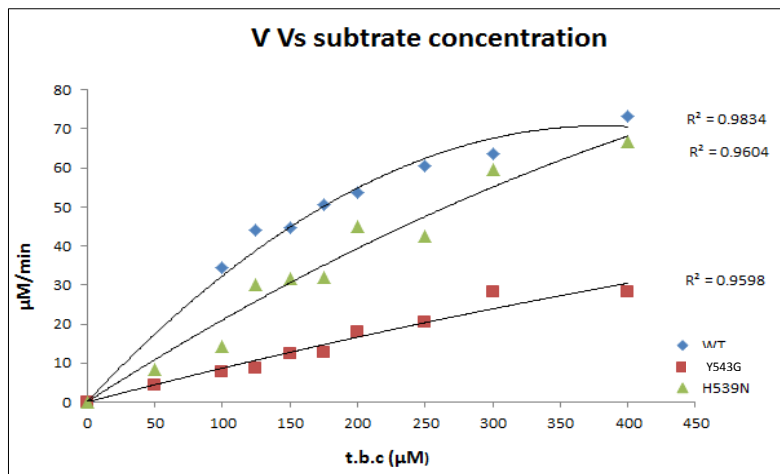
Fig. 2.13 Relationship between the substrate concentration and the initial velocity at 25 ºC. Triangles indicate the 44-kDa tyrosinase from H539N (0.0125μM); rectangulars from Y543G (0.0114μM); diamonds from WT (0.0125 μM).

2.4 Conclusion

Characteristic of *P.nameko* tyrosinase and recombinant tyrosinases are summarized in table 2.1. Cu contents of pro-form mutants (84-kDa) of WT, F515G, H539N, Y543G and L540G are 1.1, 0.8, 0.9, 1.6 and 0.1, respectively. Cu contents of 44-kDa form of WT, H539N and Y543G are 0.8, 1.4 and 0.8, respectively. On the other hand, F515G and L540G could not produce active forms of tyrosinase.

Table 2.1 Characteristics of *P.nameko* tyrosinase and recombinant tyrosinases.

Tyrosinases	Pro-form			Digested from					Character
	M.W(kDa)	Specific activity (U/mg)	Cu/molecule	M.W(kDa)	Cu/molecule	K_m (μM)	K_{cat}(s^{-1})	K_{cat}/K_m (μM^{-1}s^{-1})	
Wild type	84	0.92	1.1 *	44	0.8	189	162	0.86	Active form (Kawamura-Konishi *et al.* 2011)
Truncated Wild type	59*	-	0.1*	42*	-	-	-	-	Non-active form (Enterokinase digestion)
F515G	84	-	0.8	25	-	-	-	-	Non-active form
H539N	84	0.065	0.9 *	44	1.4	nd	nd	0.27 (tv)	Active form
Y543G	84	0.55	1.6 *	44	0.8	491	92.9	0.19	Active form
Native	67	412	-	42	2.2	163	294	1.8	Active form (Kawamura-Konishi *et al*. 2007)
L540G	84 *	-	0.1 *	25 *	-	-	-	-	Non-active form

nd ; can't be determined

tv ; tentative value

* ; the data of Saya Maekawa

In this research, we prepared four recombinant pro-tyrosinases with mutations in the vinicity of CXXC motif on the C-terminal domain of tyrosinase as the respective fusion proteins. The motif is in a highly flexible loop of the protein, and the loop can support and

block the active site of tyrosinase (Decker and Tuczek 2000; Cuff *et al*., 1998; Lerch 1982; Klabunde *et al* 1998; Merkel *et al*., 2005; Fujieda *et al*. 2013b). The experimental results suggested that Phe515, His539, L540G and Try543 residues played key functional roles in the C-terminal domain of *P. nameko* tyrosinase.

In the crystal structure of *A. oryzae* pro-tyrosinase (Fujieda *et al*. 2013b), the active site is covered by the C-terminal shielding domain, which comprises a flexible loop containing the CXXC motif. This region is completely disordered. Phe513 residue of this enzyme locates just above the dicopper active center as the placeholder and maintains the enzyme inactive. But the proteolytic digestion of the C-terminal domain having placeholder leads to opening the entrance of the active site for substrate incorporation (Fujieda *et al*. 2013b).

In contrast, Phe515 residue of *P. nameko* tyrosinase is significantly different from Phe513 of *A. oryzae*. F515G did not show activity by proteolytic digestion of the C-terminal domain, indicating that the mutant had a deforming structure. Although Phe515 did not inhibit copper insertion in the active site, it is the essential for protein folding of the N-terminal domain because the residue may locate proximity to the N-terminally in the vicinity of the flexible loop of the C-terminal domain.

Leu540 residue of *P. nameko* tyrosinase could not be activated by proteolytic digestion of the C-terminal domain. L540G had a deforming and copper-depleting structure in the N-terminal catalytic domain. These results indicated that Leu540 is the essential for protein folding of the N-terminal domain and Cu incorporation. The residue may locate in the vicinity of the flexible loop of the C-terminal domain. H539N and Y543G residues of *P. nameko* tyrosinase were activated by proteolytic digestion of the C-terminal domain, but their catalytic activities were much lower than those of the 44-kDa tyrosinase from WT and native tyrosinase. I think that these mutants affect the structure of substrate-binding pocket in the N-terminal domain but the amino acid residues of His539 and Tyr543 do not concern the inhibitory property of the C-terminal domain on the active site. The residues may locate in the vicinity of the flexible loop of C-terminal domain.

Therefore, these residues on the C-terminal domain of *P. nameko* tyrosinase are important for folding the N-terminal core domain. The residues are capable of supporting the flexible loop of the C-terminal domain and determining its orientation. Three-dimensional structure of *P. nameko* pro-tyrosinase is required to inverstigate the precise roles of the C-terminal domain.

Chapter 3
Function of the C-terminal domain of *Pholiota nameko* tyrosinase

3.1 Introduction

Generally, structure of fungal tyrosinases consist three domains: these are C-terminal domain, central (N-terminal, core) domain and linker region. All the tyrosinases have in common a binuclear type 3 copper centre within their active sites. The N-terminal active site has two copper binding motif with each three conserved histidine residues (Hatcher and Karlin 2004; Rosenzweig and Sazinsky 2006; Decker and Terwilliger, 2000). In fungal tyrosinases, two sequence motifs have been identified in the proximity of the cleavage region between the core domain and the C-terminal domain. First tyrosine motif (YXY) that is highly conserved and it interacts with the N-terminal extremity of the globular core in the three-dimensional structure, and second is tyrosine-glycine motif (YG). Moreover, conserved cysteine (CXXC) motif locates on the C-terminal domain and it is a crual motif for copper inserting into the active site *via* a thiroether linkage of CuA site. This mediation is governed by the three cysteine residues, in which two is from the CXXC motif and the left one is from thiorether linkage at the CuA site. The detail mechanism of the insertion is presented in the report of crystal structure of *A. oryzae* (Fujieda *et al.* 2013b).

The C-terminal processing domain of fungal tyrosinases has been clearly demonstrated in *Agaricus bisporus* (Wichers *et al*. 2003), *Neurospora crassa* (Kupper *et al*. 1989), *Pycnoporus sanguineus* (Halaouli *et al*. 2006b) and *Trichoderma ressei* (Selinheimo *et al*. 2006). Although the functions of C-terminal processing remain controversial, it is accepted that the active site is shielded by the C-terminal domain to maintain inactivity of the enzyme. This mechanism is reported by similarities in structures of the C-terminal domains of haemocyanins and plant polyphenol oxidases (Decker and Tuczek 2000; Decker *et al*. 2007).

3.2 Methods

The present bioinformatics programs are freely available software and were used with default parameters unless otherwise stated. Sequence alignments were performed using MAFFT (http://www.genome.jp/tools/mafft) or CLUSTALW (http://www.genome.jp/tools/clustalw). The structural presentation in Fig. 3.2 was made based on the atomic coordination data of melB *A. oryzae* tryosinase (Fujieda *et al.* 2013b) using a molecular viewer.

3.3 Results and discussion

The recombinant tyrosinase lacking the C-terminal domain had no catalytic activity; whereas the mutant L540G was copper-depleted, the other mutants had copper contents similar to that of the wild type pro-tyrosinase. Proteolytic digestion activated the mutants H539N and Y543G following release of the C-terminal domain, and the resulting tyrosinases had higher K_m values for t-butyl catechol than the wild type pro-tyrosinase. The mutants F515G and L540G were degraded by proteolytic digestion and yielded smaller proteins with no activity. The results are summarized in Table 1.

Table 3.1. Molecular mass, catalytic activity, Cu content (Cu/mol of protein) and kinetic parameters of tyrosinases.

Tyrosinase			Ms (kDa)	Chymo-trypsin	Cu content	Activity	Kinetic parameters for t-butyl catechol		
							K_m(μM)	k_{cat}(s^{-1})	k_{cat}/K_m (μM^{-1}s^{-1})
Recombinant	Mutants	F515G	84	-	0.8	-			
			25	+	nd	-			
		H539N	84	-	0.9	+			
			44	+	1.4	+	-	-	0.27
		L540G	84	-	0.1	-			
			25	+	nd	-			
		Y543G	84	-	1.6	+			
			44	+	0.8	+	491	92.9	0.19
	Wild type		84	-	1.1	+			
			44	+	0.8	+	189	162	0.86
	Lacking C-terminal domain		42	-	0.1	-			
Native			42	In vivo protease	2.2	+	163	294	1.8

Function of C-terminal domain of Pholiota nameko tyrosinase

The previous results reported that isolated a 42-kDa tyrosinase from *P. nameko* was truncated with the release of a 25-kDa C-terminal domain from an encoded 67-kDa pro-tyrosinase (Kawamura-Konishi*et al*., 2007). Subsequently, it has been shown that the recombinant pro-tyrosinase was activated by truncation of the 25-kDa C-terminal domain (Kawamura-Konishi *et al*. 2011). Therefore, it can be assumed that the C-terminal domain of the *P. nameko* pro-tyrosinase shields the active site of the enzyme and that the recombinant tyrosinase lacking of the C-terminal domain would have enzyme activity similar to that of 42-kDa tyrosinase from *P. nameko*.

In this study, I perpared a recombinant tyrosinase lacking the C-terminal domain and expressed it in *E. coli* cells as a fusion protein (Fig. 1.1, iii). Subsequent analyses revealed no evidence of enzyme activity (lane 5 in Fig. 1.2B), indicating that the C-terminal domain of *P. nameko* tyrosinase is essential for catalytic activity of the N-terminal domain. Subsequently, I performed mutagenesis study of four recombinant pro-tyrosinases carrying substituted residues on the C-terminal domain of the pro-enzyme. The results showed that Phe515 residue can affect the protein folding of the N-terminal domain; Leu540 residue can affect the copper incorporation and the protein folding of the N-terminal domain; His539 and Tyr543 residues may affect the structure of substrate-binding pocket in the N-terminal catalytic domain; their 44-kDa tyrosinases have much lower catalytic activities than that from WT pro-tyrosinase. From the results of four mutants, I assumed that these residues are important for folding the N-terminal core domain.

The function of the C-terminal domain is debated and has been ascribed to shielding over the active site and inactivating the enzyme. It is often supposed to be essential for copper incorporation and correct folding (Claus and Decker 2006; Flurkey and Inlow 2008; Fairhead and Thony-Meyer 2010). In the present study, the results showed the C-terminal domain affected the N-terminal domain of *P. nameko* tyrosinase. Because the C-terminal domain induces to construct the N-termianl active site, mutation in the residue on the C-terminal domain can procude various pro-tyrosinases possessing such properties as folded or unfolded, copper-inserted or copper-depleted, and active or inactive *etc*. Moreover, truncation of the C-terminal domain resulted in producing an inactive form. I think that the C-terminal domain of *P.nameko* tyrosinase has a chaperone-like function to produce the correct-folded structure of the N-terminal domain which brings to constructing the active site in the N-terminal domain.

At the present, three-dimensional structure of *P. nameko* tyrosinase has not been resolved yet. To understand the precise roles of the C-terminal domain, further investigations are required for the structural determination.

Prediction of three-dimensional structure of P.nameko tyrosinases

P. nameko pro-tyrosinase comprises three domains as usually shown in fungal tyrosinase. It can be found that an arginine residue is conserved in the vicinity of the N-terminus (Kawamura-Konishi *et al.* 2011). There are two catalytic binuclear copper-binding motives with each three conserved histidine residues in the N-terminal domain. Two conserved motives (YXY and YG) are also found in the proximity of the cleavage site. Moreover, cysteine motif (CXXC) locates on the C-terminal domain which has significantly lower sequence-homology than the N-terminal domain. Four mutated residues in this study are located in the vicinity of the CXXC motif on the C-terminal domain of *P. nameko* tyrosinase. The CXXC motif is crucial for Cu incorporation into the active site *via*

a thiroether linkage of CuA site. The motif located in very flexible region of the C-terminal shielding domain as predicted in reported structure of *A.oryzae* tyrosinase (Fujieda *et al.* 2013b).

At the present, three-dimensional structure of *P. nameko* has not been resolved. For understanding *P.nameko* tyrosinase, I compared amino acid sequences of *P. nameko* tyrosinase with those of the reported *A.oryzae* tyrosinase (Fujieda *et al.* 2013b) and other fungal tyrosinases. Especially, thes mutated resiudes in this study are located in the vicinity of the flexible loop containing the CXXC motif. This loop is completely disordered in the C-terminal shielding domain of the reported *A.oryzae* tyrosinase (Fujieda *et al.* 2013b). Phe454 residue of *A. bisporus* tyrosinase is also found in the flexible loop (Mauracher *et al* 2014b).

In the crystal structure of *melB* tyrosinase of *A. oryzae*, which is recently reported (Fujieda *et al.* 2013b), binuclear copper centre is buried in the cleft of the copper-binding domain and is inaccessible to the exterior solvent by hindering of the C-terminal domain. The tip of the C-terminal domain is the Phe513 residue, which phenyl ring stacks onto the imidazole ring of one of the CuB ligands. Its side chain is accommodated just above the dinuclear copper centre as the placeholder for phenolic substrates. The proteolytic digestion of the C-terminal domain having Phe513 placeholder leads to opening the entrance of the enzyme-active site for the substrate incorporation. The pro-tyrosinase composing homodimer was crystallized in apo-form and holo-form. Thioether linkage was different between the two forms. It is also concluded that the conserved Cys 92 in the Cu A site as well as the C-terminal conserved $C^{522}XXC^{525}$ motif contributes the copper incorporation in *melB* apo-pro-tyrosinase. The completely disordered region of the C-terminal domain, that is the highly flexible loop, exists near the CuA site and contains the CXXC motif within the distance range of about 5-15Å from the sulfur atom of Cys92. The authors confirmed that three cysteines (Cys92, Cys522, and Cys525) play significant roles in the copper incorporation process. The structural feature of *melB* tyrosinase suggests the action of copper chaperones. Finally they concluded that Phe513 of the C-terminal domain hinders the active site (Fujieda *et al.* 2013b).

From the present results, Phe515 residue can affect the protein folding of the N-terminal domain; Leu540 residue can affect the copper incorporation and the protein folding of the N-terminal domain; and residues of His539 and Tyr543 may affect to the structure of substrate-binding pocket in the N-terminal catalytic domain.

For understainding the structure of *P. nameko* tyrosinase, we performed sequence alignments in the fungal tyrosinases of *P. nameko*, *A. bisporus*, *L. edodoes*, *N. crassa*, *P. sanguineus* and *A. oryzae* (Fig. 3.1).

The structure of *A. oryzae* (Figs. 3.2A and B) shows that Phe513 residue locates before the flexible loop and above the dinuclear copper centre at near the CuB site and Leu534

residue locates after the flexible loop. They are away from Cu binding region. The region between the CXXC motif and Leu543 residue can not be visible in the X-ray structure due to extreme flexiblity.

On the assumption that C-terminal domain structure of *P. nameko* pro-tyrosinase is the same as that of *A. oryzae* pro-tyrosinase (Figs. 3.2C and D), Phe515 residue will be in the vicinity of the flexible loop near the N-terminally, and His539, Leu540 and Try543 will be in the vicinity of the loop of the C-terminal domain. Moreover, Phe515 residue may locate the prior to the flexible loop and near the Cu binding region and Leu540 residue may locate after the flexible loop which can support and alter the loop of the C-terminal domain even away from the Cu-binding region. Therefore, I present the conclusion that these residues can support the loop and determine its orientation. In this study, I found the importance of Leu540, which is the first report among the tyrosinase researches.

3.4 Conclusion

In this study, I first showed that the recombinant tyrosinase lacking the 25-kDa C-terminal domain is a copper deficiency and non-active form. Base on the results, I concluded that the C-terminal domain is not only inhibitor but also essential for the catalytic activity of the N-terminal domain of *P. nameko* tyrosinase.

The second results showed that the four residues of *P. nameko* tyrosinase in the C-terminal domain are important for folding of the N-terminal domain. The residues located in the vicinity of the flexible loop of the C-terminal domain can support the loop and determine its orientation.

Therefore, the C-terminal domain affects the N-terminal domain in *P. nameko* tyrosinase. It is responsible for folding, copper incorporation and catalytic activity in the catalytic N-terminal domain. I propose that the C-terminal domain of *P.nameko* tyrosinase has a chaperone-like function to produce the correct-folded structure of the N-terminal domain. Thus, I concluded that the C-terminal processing domain of *P. nameko* pro-tyrosinase is essential for correct folding of the N-terminal catalytic domain and it acts as an intramolecular chaperone during assembly of the active-site conformation.

```
                                   Conseved Arg
                                        *
P.nameko       1 M---SRVVITGVSG------TVANRLEINDFVKN-DK------FFSLYIQALQVMSSVP      43
A.bisporus     1 M---SLLATVGPTG------GVKNRLDIVDFVRD-EK------FFTLYVRALQAIQD-K      42
L.edodes       1 M---SHYLVTGATGGSTSGAAAPNRLEINDFVKQ-ED------QFSLYIQALQYIYSSK      49
N.crassa       1 MSTDIKFAITGVPTPPSSNGAVPLRRELRDLQQNYPE------QFNLYLLGLRDFQG-L      52
P.sanguineus   1 M---SHFIVTGPVGGQTEGAPAPNRLEINDFVKN-EE------FFSLYVQALDIMYG-L      48
A.oryzae      -4 GPGGSPYLITGIPKDPKH--PLPIRKDIDDWYLE-QTSAGSNRIQLTLFVEALTVIQN-R      52

                                                     Conseved Cys
                 HA1                     Cys84-His86  *  HA2           HA3
P.nameko      44 PQENVRSFFQIGGIHGLPYTPWDGITG---DQ----PFDPNTQWGGYCTHGSVLFPTWHR      96
A.bisporus    43 DQADYSSFFQLSGIHGLPFTPWAK-PK---DT----PTVP--YESGYCTHSQVLFPTWHR      92
L.edodes      50 SQDDIDSFFQIGGIHGLPYVPWDGAG----NK----PVDTD-AWEGYCTHGSVLFPTFHR     100
N.crassa      53 DEAKLDSYYQVAGIHGMPFKPWAGVPS---DTDWSQPGSS--GFGGYCTHSSILFITWHR     107
P.sanguineus  49 KQEELISFFQIGGIHGLPYVAWSDAGA---DD----PAEP----SGYCTHGSVLFPTWHR      97
A.oryzae      53 PLNDQLSYFRLAGIHGAPWTEWDGVPGGQKDS----KGNP---TGFCVHNNYTFPTWHR     104
                                                  Cys92-His94 (a thioether bridge of A. oryzae)

P.nameko      97 PYVLLYEQILHKHVQDIAATYTTSD---KAAWVQAAANLRQPYWDWAA------------     141
A.bisporus    93 VYVSIYEQVLQEAAKGIAKKFTV-H---KKEWVQAAEDLRQPYWDTGF------------     136
L.edodes     101 PYVLLIEQAIQAAAVDIAATYIV-D---RARYQDAALNLRQPYWDWAR------------     144
N.crassa     108 PYLALYEQALYASVQAVAQKFPV-EGGLRAKYVAAAKDFRAPYFDWAS---------QPP     157
P.sanguineus  98 PYVALYEQILHKYAGEIADKYTV-D---KPRWQKAAADLRQPFWDWAK------------     141
A.oryzae     105 VYVTLYEQVIYEAMLDFIKQNVPQNG--KADWENEAKQWRLPYWDFARFARHGHDNTQGD     162

P.nameko     142 -NAVPPDQVIASKKVTITGSNGHKVEVDNPLYHYKFHPIDSS----------------     182
A.bisporus   137 -ALVPPDEIIKLEQVKITNYDGTKITVRNPILRYSFHPIDPS----------------     177
L.edodes     145 -NPVPPPEVISLDEVTIVNPSGEKISVPNPLRRYTFHPIDPS----------------     185
N.crassa     158 KGTLAFPESLSSRTIQVVDVDGKTKSINNPLHRFTFHPVNPS--------------PGD     202
P.sanguineus 142 -NTLPPPEVISLDKVTITTPDGQRTQVDNPLRRYRFHPIDPS----------------     182
A.oryzae     163 ELRLPILVTMPMVKVLVPGQPGKQLSKPNPLYRFQMQTLMGTLERPYAITSQKTEEHGWS     222

P.nameko     183 FP--RPYSEWPTTLRQPNSSRPNATDNVAKLRNVLRA----------------SQENIT     223
A.bisporus   178 FSGYPNFDTWRTTVRNP---DADKKENIPALIAKLDL----------------EADSTR     217
L.edodes     186 FP--EPYQSWSTTLRHPLSDDANASDNVPELKATLRS----------------AGPQLK     226
N.crassa     203 FS--AAWSRYPSTVRYPNRLTGASRD--ERIAPILAN----------------ELASLR     241
P.sanguineus 183 FP--EPYSNWPATLRHPTSDGSDAKDNVKDLTTTLKA----------------DQPDIT     223
A.oryzae     223 FD--LPFDKCQSTTKYGLLENYNADVWADGGQNWLRANLALNEHPWYQNLDGWDSVPTLQ     280

                                                              HB1   HB2
P.nameko     224 SNTYSMLTRVH-TWKAFS------NHTVGDGGSTSN-----------SLEAIHDGIHVD     264
A.bisporus   218 EKTYNMLKFNA-NWEAFS------NHGEFD-DTHAN-----------SLEAVHDDIHGF     257
L.edodes     227 TKTYNLLTRVH-TWPAFS------NHTPDDGGSTSN-----------SLEGIHDSVHVD     267
N.crassa     242 NNVSLLLLSYK-DFDAFSYNRWDPNTNPGDFG---------------SLEDVHNEIHDR     284
P.sanguineus 224 TKTYNLLTRVH-TWPAFS------NHTPGDGGSSSN-----------SLEAIHDHIHDS     264
A.oryzae     281 DMTFRLLTTGGLNWGEFS------STRYDDKKEETQPKNNEQAPKNWMNLEAIHNNVHNW     334

                                                    HB3
P.nameko     265 VG--------------GG---GHMADPAVAAFDPIFFLHCNVDRLLSLWAAINPGVWV     306
A.bisporus   258 VG--------------RGAIRGHMTHALFAAFDPIFWLHSNVDRHLSLWQALYPGVWV     302
L.edodes     268 VG--------------GN---GQMSDPSVAGFDPIFFMHAQVDRLLSLWSALNPRVWI     309
N.crassa     285 TG--------------GN---GHMSSLEVSAFDPLFWLHVNVDRLWSIWQDLNPNSFM     326
P.sanguineus 265 VG--------------GG---GQMGDPSVAGFDPIFFLHCQVDRLLALWSALNPGVWV     306
A.oryzae     335 VGGFMFSRPGRHDLKLWGA---GHMSSVPVAAYDPIFWLHCNIDRLTAIWQTVNSGSWF     391

                                                             YXY motif
P.nameko     307 SPGDSEDGTFILPPEAPVDVSTPLTPFS-----NTETTFWAS--GGITDTTKLGYTYPEF     359
A.bisporus   303 TQGPEREGSMGFAPGTELNKDSALEPFY-----ETEDKPWTS--VPLTDTALLNYSYPDF     355
L.edodes     310 TDGPSGDGTWTIPPDTVVGKDTDLTPFW-----NTQSSYWIS--ANVTDTSKMGYTYPEF     362
N.crassa     327 TPRPAPYSTFVAQEGESQSKSTPLEPFW----DKSAANFWTS--EQVKDSITFGYAYPET     380
P.sanguineus 307 NSSSSEDGTYTIPPDSTVDQTTALTPFW-----DTQSTFWTSFQSAGVSPSQFGYSYPEF     361
A.oryzae     392 NDDKSK----------VSKDDDLRPFHRFCEKTRKVVFFRS--DDVKDWRSLNYDYAIT     438
```

37

```
                       YG motif              Cleavage site
                                                  ↓
P.nameko      360 NGLDLGNAQAVKAAIGNIVNRLYGASVFSGF---------AAATSAIGAGSVASLAADV-   409
A.bisporus    356 DKVKGGTPDLVRDYINDHIDRRYGIKKSEGG----------KNPALDLLSDFKGV----   400
L.edodes      363 NNLDMGNEVAVRSAIAAQVNKLYGGPFTKFA--------AAIQQPSSQTTADASTIGNV-   413
N.crassa      381 QKWKYSSVKEYQAAIRKSVTALYGSNVFANFVENVADRTPALKKPQATGEESKSTVSAAA   440
P.sanguineus  362 NGLNLQDQKAVKDHIAEVVNELYGHRMRKTF---------PFPQLQAVSVAKQGDAV-   409
A.oryzae      439 KD--------ASRIRKEISDLYGQRTKEVY----------------------------   460
                                                  ↑
                                            Proteolytic site of A. oryzae

P.nameko      410 -----------------------PLEKAPAPAPEAAAQSPVPAPAHVEPAVRAVSVHA   444
A.bisporus        --------------------------------------------------------
L.edodes      414 ------------------------TSDASSHLVDSKINPTP--------------   430
N.crassa      441 AHAVELSGAKKVAEKVHNVFQHAEEKAQKPVVPVKDTKAESSTAAGMMIGLSIKRPSKLT   500
P.sanguineus  410 -----------------------------TPSVATDSVSSSTTPAE---NPASR-----E   432
A.oryzae          --------------------------------------------------------

P.nameko      445 AAAQPHAEPPVHV---SAGGHPSPHGFYDWTARIEFKKYEFGSS-FSVLLFLGPVPEDPE   500
A.bisporus    401 ---------------THDHNEDLKMFDWTIQASWKKFELDDS-FAIIFYFA---ADGS   439
L.edodes      431 ---NRSIDDAPQVKIASTLRNNEQKEFWEWTARVQVKKYEIGGS-FKVLFFLGSVPSDPK   486
N.crassa      501 ASPGPIPESLKYLA--------PDGKYTDWIVNVRAQKHGLGQS-FRVIVFLGEFNPDPE   551
P.sanguineus  433 DASDKDTEPTLNVEVAAPGAHLTSTKYWDWTARIHVKKYEVGGS-FSVLLFLGAIPENPA   491
A.oryzae      461 --------------------KDFGEEDYILSIRYSRYALGGKPFQINIFFGDVDGKDF   498

                   F515                 CXXC motif              H539 L540 Y543
                    #                                             ## #
P.nameko      501 QWLVSPNFVGAHHAFVNS-AAGHCANCR--NQGNVVVEGFVHLTKYISEH---AGLRSLN   554
A.bisporus    440 TNVTKENYIGSINIFRGT-TPTNCANCR--TQDNLVQEGFVHLDRFIARD-----LDTFD   491
L.edodes      487 EWATDPHFVGAFHGFVNS-SAERCANCR--RQQDVVLEGFVHLNEGIANI---SNLNSFD   540
N.crassa      552 TWDDEFNCVGRVSVLGRS-AETQCGKCRKDNANGLIVSGTVPLTSALLQDIVGGELQSLK   610
P.sanguineus  492 DWRTSPNYVGGHHAFVNS-SPQRCANCR--GQGDLVIEGFVHLNEAIARH---AHLDSFD   545
A.oryzae      499 YDARSQNFVGSVFNFSGSLEDSNCDKCA--QQEQEGVLSVSQLPARLAVH---YYKKQNK   553
                      Phe513    ---------------- Flexible loop in C-terminal domain of A. oryzae

P.nameko      555 PEVVEPYLT-NELHWRVLKADGSVGQLE---SLEVSVYGTPMNLPVGAMFP-----VP--   603
A.bisporus    492 PQAVHRYLKEKKLSYKVVADDHSVT----LKSLRIRVQGRPLHLPPGVSFPRLDKNIPIV   547
L.edodes      541 PIVVEPYLK-ENLHWRVQKVSGEVVNLDAATSLEVVVVATRLELPPGEIFP-----VP--   592
N.crassa      611 PEDVIPHLR-ANLKWKVALFNGDEYNLEEVPDLKVSVASTEVTIDEEGLPH-----YS--   662
P.sanguineus  546 PTVVRPYLT-RELHWGVMKVNGTVVPLQDVPSLEVVVLSTPLTLPPGEPFP-----VP--   597
A.oryzae      554 GEVPTP-------RYVVVNSQGKA-----EAEVKVEV---ALHKTEGTFYD-----AP--   591

P.nameko      604 --------------------------------------------GNRRHFHGITHGRVGGS   620
A.bisporus    548 NFDDVLDLVTGVVNIGLTAVGATAGVAIGVVGATAGTAIGVAGAATDAVTNIAKGGLGAL   607
L.edodes      539 --------------------------------------------AETHHHHHITHGRPGGS   609
N.crassa      663 --------------------------------------------RQYTVYPEITEGKPCGH   679
P.sanguineus  598 --------------------------------------------GTPVNHHDITHGRPGGS   614
A.oryzae      592 --------------------------------------------ARGGSDDYRRVADGKRAEV   615

P.nameko      621 RHAIV----   625
A.bisporus    608 GRIF-----   611
L.edodes      610 RHSVASSSS   618
N.crassa      680 GPEDH---I   685
P.sanguineus  615 HHTH-----   618
A.oryzae      611 DDAYR---A   616
```
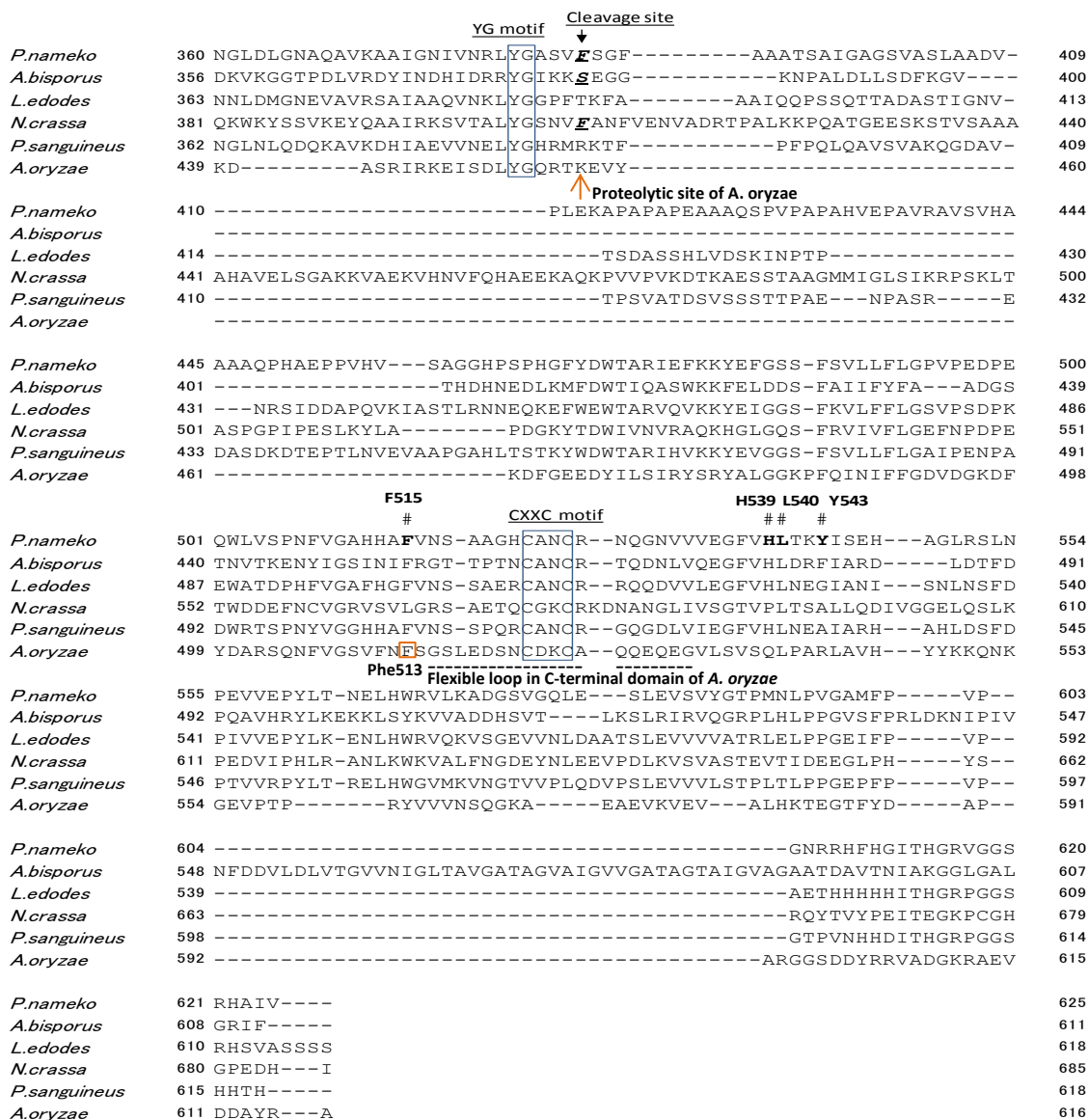
Fig. 3.1 Multiple sequence alignment of amino acid sequences from fungal tyrosinases. Base on the fungal tyrosinase, *A. oryzae* (Fujieda *et al*. 2013b).The alignment was generated using the MAFFT service in DDBJ. Copper ligands of the six conserved histidine residues of fungal tyrosinase are represented in boldface (HA1, HA2 and HA3 for CuA and HB1, HB2 and HB3 for CuB). Highly conserved sequences (YXY motif, YG motif and CXXC motif) are boxed. Conserved Arg and conserved Cys are marked with asterisks. The arrow represents the proteolytic cleavage site and its reported corresponding residues (Flurkey and Inlow 2008) are underlined in bold italics. Point mutated amino acid residues F515, H539, L540 and Y543 are marked with sharp signs; *P. nameko*, tyr2 from *Pholiota*

nameko (AB275647); *A. bisporus*, PPO4 from *Agaricus bisporus* (C7FF05); *L. edodes*, *Lentinula edodes* (BAB71735); *N. crassa*, *Neurospola crassa* (CAE81941); *P. sanguineus*, *Pycnoporus sanguineus* (AAX46018.1); *A. oryzae*, *melB* from *Aspergillus oryzae* (3W6W_B).
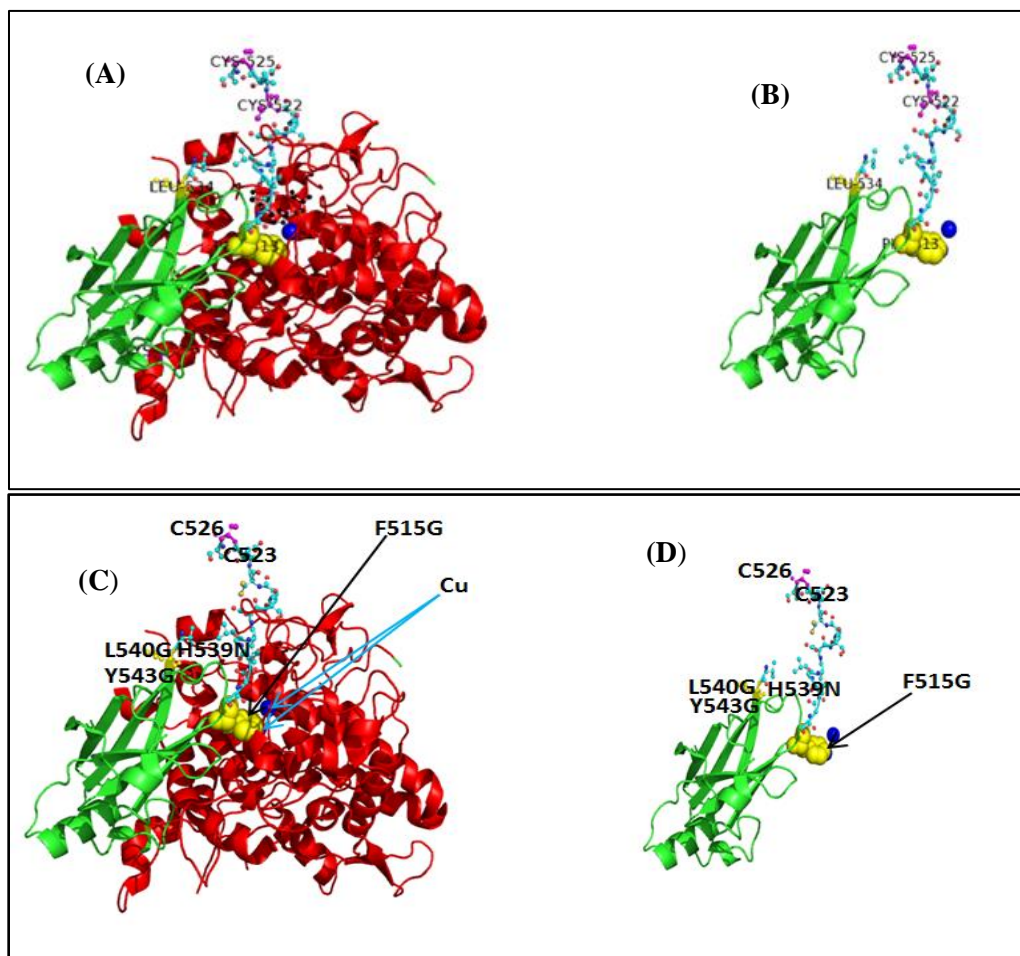

Fig. 3.2 Structure of *melB A. oryzae* tyrosinase (Fujieda *et al*. 2013b). (A and C): Crystal structure of *melB A. oryzae* pro-tyrosinase (Fujieda *et al*. 2013b); (B and D): C-terminal domain of the *melB* pro-tyrosinase; (C and D): residual numbers of *P. nameko* tyrosinase are superimposed on the structure of the *melB* pro-tyrosinase on the assumption that *P. nameko* tyrosinase has the same structure of the *melB* pro-tyrosinase. Red color indicates the N-terminal domain, green color indicates the C-terminal domain, and yellow color indicates the phenyl ring of Phe513 in the *melB* pro-tyrosinase and Phe515 in *P. nameko* tyrosinase.

SUMMARY AND CONCLUSION

Tyrosinase (EC 1.14.18.1) is a type-3 copper protein, containing a binuclear copper centre in the active site. Tyrosinase uses molecular oxygen to catalyse the *ortho*-hydroxlation of monophenols and the subsequent oxidation of *o*-diphenols. The resulting *o*-quinones are highly reactive compounds that polymerize non-enzymatically to form melanin pigments. Tyrosinase is of interested to the food industry in the improvement of food as to flavour, taste and texture by polymerization of phenol derivatives and by cross-linking of protein-protein and protein-polysaccharide complexes. Tyrosinase from edible mushrooms is especially expected to have biotechnological potential in food applications because the non-toxicity of the tyrosinase is certified by historical use of mushrooms as a food.

Pholiota nameko (nomenclature *Pholiota microspore*) has a high level of tyrosinase activity among edible mushrooms. *P. nameko* tyrosinase is expressed as a latent 67-kDa pro-enzyme protein and is converted to an active 42-kDa mature-enzyme that is cleaved with a C-terminal 25-kDa polypeptide from the 67-kDa protein. Thus, the C-terminal cleavage activates the N-terminal 42-kDa domain, suggesting a possibility that the C-terminal domain may acts as an inhibitor in the pro-enzyme. To investigate the function of the pro-enzyme C-terminal processing domain of *P. nameko* tyrosinase, a recombinant tyrosinase lacking the C-terminal domain was expressed in *Eschericia coli* cells and mutagenesis studies were performed on the C-terminal domain of a recombinant pro-tyrosinase.

Using the oligonucleotide-directed mutagenesis method, four mutants were prepared: F515G (Phe515 was substituted with Gly), H539N (His539 was substituted with Asn), L540G (Leu540 was substituted with gGly) and Y543G (Tyr543 was substituted with Gly). Recombinant proteins were expressed as thioredoxin fusion proteins and purified by ammonium sulfate precipitation and column chromatography. Recombinant pro-tyrosinases were digested with bovine pancreatic α-chymotrypsin to be 44-kDa tyrosinases cleavaged with the C-terminal domain. Protein concentrations were determined using the Bradford method. Recombinant proteins were assayed using SDS-PAGE without boiling or reducing agents and enzyme activity on the gel was visualized with tyramine and 3-*methyl*-2-benzo-thiazolinone hydrochloride hydrate. For western blotting, protein bands from gels were electro-transferred onto polyvinyliodine fluoride membranes and the membranes were reacted with rabbit polyclonal antibodies against tyrosinase from fruiting bodies of *P. nameko* or the peptide PVPGNRRHFHGIT followed by incubation with peroxidase-

conjugated secondary goat anti-rabbit Immunoglobulin G. Kinetic parameters of tyrosinase reaction were obtained by assaying the enzyme activity for 4-*t*-butylcatechol.

The recombinant tyrosinase lacking the C-terminal domain had no catalytic activity; whereas the mutant L540G was copper-depleted, the other mutants had copper contents similar to that of the wild type pro-tyrosinase. Proteolytic digestion activated the mutants H539N and Y543G following release of the C-terminal domain, and the resulting tyrosinases had higher K_m values for *t*-butyl catechol than the wild type pro-tyrosinase. The mutants F515G and L540G were degraded by proteolytic digestion and yielded smaller proteins with no activity.

The results suggest that the C-terminal processing domain of *P. nameko* pro-tyrosinase is essential for correct folding of the N-terminal catalytic domain, and acts as an intramolecular chaperone during assembly of the active-site conformation.

REFERENCES

Aberg, C. M., Chen, T., Olumide, A., Raghavan, S. R., and Payne, G. F. (2004) Enzymatic grafting of peptides from casein hydrolysate to chitosan. Potential for value addedby-products from food-processing wastes. *J Agric Food Chem* **52**: 788-793.

Cabrera-Valladares, N., Martinez, A., Pinero, S., Lagunasmunoz, V., Tinoco, R., Deanda, R., vazquezduhalt, R., Bolivar, F., and Gosset, G. (2006) Expression of the melA gene 79 from *Rhizobiumetli* CFN42 in *Escherichia coli* and characterization of the encoded tyrosinase. *Enzyme and Microbial Technology* **38**: 772-779.

Chen, T., Embree, H. D., Wu, L. Q., and Payne, G. F., (2002) In vitro protein-polysaccharide conjugation: tyrosinase-catalyzed conjugation of gelatin and chitosan. *Biopolymers* **64**: 292-302.

Claus, H., and Decker, H. (2006) Bacterial tyrosinases. *Systematic and Applied Microbiology* **29**: 3-14.

Cuff, M. E., Miller, K. I., van Holde, K. E., and Hendrichson, W. A. (1998) Crystal structure of a functional unit from *Octopus* hemocyanin. *journal of Molecular Biology* **278**: 855-870.

Decker, H., Schweikardt, T., Nillus, D., Salzbrunn, U., Jaenicke, E., and Tuczek, F. (2007) Similar enzyme activation and catalysis in hemocyanins and tyrosinases. *Gene* **398**: 183-191.

Decker, H., and Tuczek, F. (2000) Tyrosinase/catecholoxidase activity of hemocyanins: structural basis and molecular mechanism. *TIBS* **25**: 392-397.

Decker, H., and Terwilliger, N., Review; Cops and Robbers (2000) Putative Evolution of Copper Oxygen-binding proteins. *The Journal of Experimental Biology* **203**: 1777-1782.

Del Marmol, V., and Beermann, F. (1996) Tyrosinase and related proteins in mammalian pigmentation. *FEBS Letters* **381**: 165-168.

Eicken, C., Krebs, B., and Sacchettini, J. C. (1999) Catechol oxidase-structure and activity. *Curr. Opin. Struct. Biol* **9**: 677-683.

Espín, J. C., Morales, M., García-Ruiz, P. A., Tudela, J., and García-Cánovas, F. (1997) Improvement of a continuous spectrophotometric method for determining the monophenolase and diphenolase activities of mushroom polyphenol oxidase. *J Agric Food Chem* **45**: 1084-1090.

Espín, J. C., and Wicher, H. J. (1999) Activation of a latent mushroom (*Agaricus bisporus*) tyrosinase isoform by sodium dodecyl sulfate (SDS). *J Agric Food Chem* **47**: 3518-3525.

Faccio, G., Arvas, M., Thony-Meyer, L. (2013) Experimental and bioinformatic investigation of the proteolytic degradation of the C-terminal domain of a fungal tyrosinase. *J.Inor.biochem* **12**: 37-45.

Fairhead, M., and Thony-Meyer, L. (2010) Role of the C-terminal extension in a bacterial tyrosinase. *FEBS journal* **277**: 2083-2095.

Fenoll, L. G., Penalver, M. J., and Rodríguez-López, J. N, (2004) Tyrosinase kinetics: Discrimination between two models to explain the oxidation mechanism of monophenol and diphenol substrates. *Int.J.Biochem* **36**: 235-246.

Flurkey, W. H., and Inlow, J. K. (2008) Proteolytic processing of polyphenol oxidase from plants and funji. *J Inorg Biochem* **102**: 2160-2170.

Freddi, G., Anghileri, A., Sampaio, S., Buchert, J., Monti, P., and Taddei, P. (2006) Tyrosinase-catalyzed modification of Bombyx mori silk fibroin: grafting of chitosan under heterogeneous reaction conditions. *J Biotechnol* **125**: 281-294.

Fujieda, N., Murata, M., Yabuta, S., Ikeda, T., Shimokawa, C., Nakamura, Y., Hata, Y., and Itoh, S., (2013a) Activation mechanism of melB tyrosinase from Aspergillus oryzae by acidic treatment. *J Biol Inorg Chem* **18**: 19-26.

Fujieda, N., Yabuta, S., Ikeda, T., Oyama, T., Muraki, N., Kurisu, G., and Itoh, S. (2013b) Crystal Structure of Copper-depleted and Copper-bound Fungal Pro-tyrosinase. *The Journal of Biological Chemistry* **288**: 22128-22140.

Garcia-Borron, J. C., and Solano, F. (2002) Molecular anatomy of tyrosinase and its related proteins: beyond the histidine-bind metal catalytic center. *Pigment Cell Res* **15**: 162-173.

Haghbeen, K., and Tan, E. W. (2003) Direct spectrophotometric assay of monooxygenase and oxidase activities of mushroom tyrosinase in the presence of synthetic and natural substrates. *Anal. Biochem* **312**: 23-32.

Halaouli, S., Asther, M., Sigoillot, J. C., Hamdi, M., and Lomascolo, A. (2006) Fungal tyrosinases: new prospects in molecular characteristics, bioengineering and biotechnological applications. *J Appl Microbiol* **100**: 219-232.

Halaouli, S., Asther, Mi., Kruus, K., Guo, L., Hamdi, M., Sigoillot, J.C., Asther, M. and Lomascolo (2005) Characterization of a new tyrosinase from *Pycnoporus* species with high potential for food technological applications. *J Appl Microbiol* **98**: 332-343.

Halaouli, S., Record, E., Casalot, L., Hamdi, M., Sigollot, J. C., Asther, M., and Lomascolo, A. (2006b) Cloning and characterization of a tyrosinase gene from the white-rot fungus Pycnoporus sanguineus, and over reproduction of the recombinant protein in *Aspergillus niger*. *Appl Microbiol Biotechnol* **70**: 580-589.

Hatcher, L. Q., and Karlin, K. D. (2004) Oxidant types in copper-dioxygen chemiatry: the ligand coordination defines the Cu_π-O_2 structure and subsequent reactivity. *J Biol Inorg Chem* **9**: 669-683.

Hearing, V. J., and Tsukamoto, K. (1991) Enzymatic control of pigmentation in Mammals. *FASEB J* **5**: 2902-2909.

Hurrell, R. F. and Finot, P. A. (1982) Protein-polyphenol reactions. 1. Nutritional and metabolic consequences of the reaction between oxidized caffeic acid and the lysine residues of casein. *Br JNutr* **47**: 191-211.

Ismaya, W. T., Rozeboom, H. J., Weijn, A., Mes, J. J., Fusetti, F., Wichers, H. J., and Dijkstra, B. W. (2011) Crystal Structure of Agaricus bisporus Mushroom Tyrosinase: Identity of the Tetramer Subunits and Interaction with Tropolone. Wageningen University and Research Center, Wageningen, *The Netherlands, Biochemistry* **50**: 5477-5486.

Jolivet, S., Arpin, N., Wichers, H. J., and Pellon, G. (1998) *Agaricus bisporus* browning: a review. *Mycol. Res.* **102**: 1459-1483.

Kawamura-Konishi, Y., Tsuji M, Hatana S, Asanuma M, Kakuta D, Kawano T, Mukouyama E.B, Goto H and Suzuki H (2007) Purification, Characterization, and Molecular Cloning of tyrosinase from Pholiota nameko. *Biosci. Biotechnol. Biochem* **71**: 752-1760.

Kawamura-Konishi, Y., Maekawa, S., Tsuji, M., and Goto, H., (2011) C-terminal processing of tyrosinase is responsible for Pholiota microspora proenzyme. *Appl Microbiol Biotechnol* **90**: 227-234.

Klabunde, T., Eicken, C., Sacchettini, J. C., and Krebs, B. (1998) Crystal structure of a plant cathchol oxidase containing a dicopper center. *Nature structural biology* **5**: 1084-1090.

Kohashi, P. Y., Kumagai, T., Matoba, Y., Yamamoto, A., Maruyama, M., and Sugiyama, M. (2004) An efficient method for the overexpression and purification of active tyrosinase from *Streptomyces castaneoglobisporus*. *Protein expression and purification* **34**: 202-207.

Kupper, U., Niedermann, D.M., Travaglini, G., Lerch, K. (1989) Isolation and characterization of tyrosinase gene from *Neurospora crassa*. *J Biol Chem* **264**: 17250-17258.

Laemmli, U. K. (1970) Cleavage of structural proteins during the assembly of the head of bacteriophage T4. *Nature* **227**: 680-685.

Lantto, R., Puolanne, E., Kruus, K., Buchert, J., and Autio, K. (2007) Tyrosinase-aided protein cross-linking: effects on gel formation of chicken breast myofibrils and texture and water-holding of chicken breast meat homogenate gels. *J Agric Food Chem* **55**: 1248-1255.

Largeteau, M. L., Latapy, C., Minvielle, N., Regnault-Roger, C., and Savoie, J. M. (2010) Expression of phenol oxidase and heat-shock genes during the development of *Agaricus bisporus* fruiting bodies, healthy and infected by *Lecanicillium fungicola*. *Appl Microbiol Biotechnol* **85**: 1499-1507.

Lerch, K., (1982) Primary structure of tyrosinase from *Neurospora crassa*. *The journal of biological chemistry* **257**: 6414-6419.

Li, Y., Wang, Y., Jiang, H., and Deng, J., (2009) Crystal structure of Manduca sexta prophenolocidase provides insights into the mechanism of type 3 copper enzymes. *Proc Natl Acad Sci USA* **106**:17002-17006.

Matoba, Y., Kumagi, T., Yamamoto, A., Yoshitsu, H., and Sugiyama, M. (2006) Crystallographic Evidence That the Dinuclear Copper Center of Tyrosinase is Flexible during Catalysis. *The journal of Biological Chemistry* **28**: 8981-8990.

Mauracher, S. G., Molitor, C., Michael, C., Kragl, M., Rizzi, A., and Rompel, A. (2014a) High level protein- purification allows the unambiguous polypeptide determination of latent isoform PPO4 of mushroom tyrosinase. *Phytochem* **99**: 14-25.

Mauracher, S. G., Molitor, C., Al-Oweini, R., Kortz, U., and Rompel, A. (2014b) Latent And active *ab*PPO4 mushroom tyrosinases cocrystallized with hexatungstotellurate(VI) in asingle crystal. *Acta Cryst Sect* D **70**: 2301-2315.

Merkel, M., Moller, N., Piacenza, M., Grimme, S., Rompel, A., and Krebs, B. (2005) Less symmetrical dicopper (II) complexes as catechol oxidase models-an adjacent thioether group increases catecholase activity. *Chemistry* (Weinheim and der Bergstrasse, Germany) **11**: 1201-1209.

Moore, J. T., Uppal, A., Maley, F., and Maley, G. F. (1993) Overcoming inclusion body formation in a high-level expression system. *Protein Expr Purif* **4**: 160-163.

Nakamura, M., Nakajima, T., Ohba, Y., Yamauchi, S., Lee, B. R., and Ichishima, E. (2000) Identification of copper ligands in *Aspergillus oryzae* tyrosinase by site-directed mutagenesis. *Biochem J* **360**: 537-545.

Narayan, A. V., and Agrawal, P. (2012) Enzyme based process for removal of phenol from waste water: Current status and future challenges. *J Environmental Research and Development* **7**: 724-728.

Neda, H. (2008) Correct name for "nameko". *Mycoscience* **49**: 88-91.

Rodriguez-Lopez, J. N., Tudela, J., and Varon, R. (1992) Analysis of a kinetic model for melanin biosynthesis pathway. *J. Biol. Chem* **267**: 3801-3810.

Rosenzweig, A. C., and Sazinsky, M. H. (2006) Structural insights into dioxygen-activating copper enzymes. Curr. Opin. Struct. *Biol* **45**: 15392-15404.

Selinheimo, E., Saloheimo, M., Ahola, E., Westerholm-Parvalen, A., Kalkkinen, N., Buchert, J., and Kruus, K., (2006) Production and characterization of a secreted, C-

terminally processed tyrosinase from the filamentous fungus *Trichoderma reesei*. *FEBS J* **273**: 4322-4335.

Selinheimo, E., Autio, K., Kruus, K., and Buchert, J. (2007a) Elucidating themechanism of laccase and tyrosinase in wheat bread making. *J Agric Food Chem* **55**: 6357-6365.

Selinheimo, E., NiEidhin, D., Steffensen, C., Nielsen, J., Lomascolo, A., Halaouli, S., Record, E., O'Beirne, D., Buchert, J., and Kruus, K. (2007b) Comparison of the characteristics of fungal and plant tyrosinases. *J Biotechnol* **130**: 471–480.

Sendovski, M., Ben-Yosef, V. S., Adir, N., and Fishman, A. (2011) First structures of an active bacterial tyrosinase reveal copper plasticity. *Journal of Molecular Biology* **405**: 227-237.

Seo, S. Y., Sharma, V. K., Sharma, N. (2003) Mushroom tyrosinase: recent prospects. *J Agric Food Chem* **51**: 2837-2853.

Solano, F., Briganti, S., Picardo, M., Ghanem, G. (2006) Hypopigmenting agents: an updated review on biological, chemical and clinical aspects. *Pigment Cell Res* **19**: 550-571.

Soler-Rivas, C., Jolivet, S., Arpin, N., Olivier, J. M., Wichers, H. J. (1999) Biochemical and physiological aspects of brown blotch disease of *Agaricus bisporus*. *FEMS Microbiology Reviews* **23**: 591-614.

Solomon, E. I., Sundaram, U. M., and Machonkin, T. E. (1996) Multicopper Oxidases and Oxygenases. *Chem. Rev* **96**: 2563-2605.

Sugumaran, M. (2002) Comparative biochemistry of eumelanogenesis and the protective roles of phenoloxidase and melanin in insects. *Pigment Cell Res* **15**: 2-9.

Thalmann, C. R., and Lötzbeyer, T. (2002) Enzymatic cross-linking of proteins with tyrosinase. *Eur Food Res Technol* **214**: 276-281.

Wang, N., and Hebert, D. N. (2006) Tyrosinase maturation through the mammalian secretory pathway: bringing colour to life. *Pigment Cell Res* **19**: 3-18.

Weaver, R. F., Rajagopalan, K. V., Handler, P., Jeffs, P., Byrne, W. L., and Rosenthal, D. (1970) Isolation of γ-L-glutaminyl 4-hydroxybenzene and γ-L-glutaminyl 3,4-benzoquinone: a natural sulfhydryl reagent, from sporulating gill tissue of the mushroom *Agaricus bisporus*. *Proc Natl Acad Sci USA* **67**: 1050-1056.

Westerhof, W. (2006) The discovery of the human melanocyte. *Pigment Cell Res* **19**: 183-193.

Wichers, H. J., Recourt, K., Hendriks, M., Ebbelaar, C. E., Biancone, G., Hoeberichts, F. A., Mooibroek H and Soler-Rivas C. (2003) Cloning, expression and characterisation of two tyrosinase cDNAs from *Agaricus bisporus*. *Appl Microbiol Biotechnol* **61**: 336-141.

LIST OF PUBLICATION

1. Moe, L. L., Maekawa, S., and Kawamura-Konishi, Y. (2015) The pro-enzyme C-terminal processing domain of *Pholiota nameko* tyrosinase is responsible for folding of the N-terminal catalytic domain. *Appl. Microbiol. Biotechnol.*, *in press*.

ACKNOWLEDGEMENTS

First and foremost I would like to express my special thanks to the president of Ishikawa Prefectural University for accepting this training course. Moreover, this acknowledgement is dedicated to my Supervisor, Prof. Yasuko Kawamura-Konishi (Department of Food Analysis, IPU) and I will keep the invaluable advice, instruction and teaching as a good guide of my Prof. in the bottom of my heart during in my school days in here. If I did not get any good instructions and guidance of my supervisor, the thesis cannot be finished in time. I therefore do appreciate and treasure my supervisor.

Let me express acknowledgement of my academic years to Prof. Toshihiro Yano (Food Management) and Prof. Takamoto Suzuki (Food Hygiene) who retired from IPU in March, 2014, and associated Prof. Yoshitsugu Nakaguchi (Food Management) and associated Prof. Sogo Nishimoto (Food Hygiene) for their suggestions and comments on during my seminar times.

In addition, I will never forget Prof. Hideyuki Goto (Biochemistry) for kindly allow me to use the Biochemistry textbook and lab accessory whenever I need.

Furthermore, earliest days of my daily life in your esteemed country, Japan, let me frankly say, I got hard days and finally I settled in here very quickly as I got invaluable suggestion and warmly cooperation from Prof. Toshiki Enomoto (Food Chemistry). Therefore I want to express my deeply thanks to Prof. Toshiki Enomoto. Moreover, I would like to highlight my gratitude to Associated Prof. Takashi Koyanagi (Food Microbiology) for providing the software what I need.

Continuously I want to mention my thanks to all Professors and Associated/Assistant Professors from IPU for giving a precious time to all my research presentations. I also want to appreciate that I got some data in related with my research from Ms. Saya Maekawa she was a master student of IPU. And thanks to my lab's member and all my friends for their delighted help.

Especially, I would like to express my gratitude to Japan International Cooperation Agency (JICA) for giving the chance to learn the great course at IPU, Japan as a scholarship "Ph.D degree in food Science and Technology: Bio-resources and environmental sciences" and I dare say I never forget Director, associated/assistant Director and Coordinator who are responsible for this training course for giving a lot of help, advice and remarkable hospitality to me. I do appreciate and would like to say thank you all on behalf of my family and my country.

In sum, I would like to express special thanks to my mother unit, the Ministry of Commerce for giving a chance to attend the great course. I wish to respect to all teachers along my life for sharing great knowledge and guidance, and a special thanks to Ex. Prof. U

Win (Biology, Yangon University), assistant lecturer Dr. Ohmar Than (Botany, Yangon University).

Finally, I would like to mention special thanks to my parents and my family for their motivation, encouragement and kindly understand to me.